Enclaves and their bearing on the origin of the Cornubian batholith, southwest England

JAMES A. STIMAC

Earth and Environmental Sciences, MS-D462, Los Alamos National Laboratory, Los Alamos, New Mexico 87545, USA

ALAN H. CLARK AND YANSHAO CHEN*

Department of Geological Sciences, Queen's University, Kingston, Ontario, Canada K7L 3N6

AND

SAMMY GARCIA

INC-15, MS-G776, Los Alamos National Laboratory, Los Alamos, New Mexico 87545, USA

Abstract

Enclaves of diverse origin are present in minor amounts in the coarse-grained biotite granites of the Cornubian batholith, southwest England. The most common enclave type is layered, rich in biotite, cordierite and aluminosilicates, and has textures and compositions that reveal variable degrees of melt extraction from metasedimentary source rocks. Rare sillimanite-bearing enclaves represent residual material, either from the region of magma generation or its ascent path, but most such enclaves were probably derived from the contact aureole closer to the present level of exposure. These non-igneous enclaves (NIE) and their disaggregation products are present in all major plutons, comprising from < 2 to 5 vol.% of the granites. Enclaves of igneous origin are also present in all major plutons except Carnmenellis, generally comprising < 1 vol.% of the granites. The most common type is intermediate in composition, with microgranular texture, and mineral compositions and textures consistent with an origin by magma mixing. Large crystals of K-feldspar, plagioclase and quartz, common in these microgranular enclaves (ME) but absent in NIE, represent phenocrysts derived from the silicic end-member during magma mixing events rather than products of metasomatism as suggested previously. Although the composition of the mafic end-member (basaltic or lamprophyric) involved in the mixing process is poorly constrained, the presence of ME in the granites, and the preponderance of mantle-derived mafic rocks in the coeval Exeter Volcanics, indicate that mafic magma injection into the crust was a factor in the generation of the batholith. Advection of sub-crustal heat provides an explanation for large-volume crustal melting in regions of relatively thin crust such as southwest England.

KEYWORDS: enclaves, magma mixing, S-type granite, Cornubian batholith.

Introduction

ENCLAVES of diverse origin are common in granitoid rocks and provide evidence of the processes controlling or influencing their genesis (Didier, 1973; Vernon, 1983, 1990; papers in Didier and Barbarin, 1991*a*). Such enclaves are present in the coarse-grained biotite granites of the Cornubian batholith of southwest England (Ghosh, 1928; Brammall and Harwood, 1932; Lister, 1984), but have only been considered in passing in recent studies. We have examined these enclaves as part of a continuing effort to clarify the petrogenesis and intrusive history of this classic granitoid province,

* Present address: Dept. of Physics, University of Toronto, 60 St. George St., Toronto, Ontario, Canada M5S 1A7

© *Copyright the Mineralogical Society*

and of its associated world-class Sn-Cu mineralization (Chen *et al.*, 1993; Clark *et al.*, 1993). In this contribution we summarize the results of a systematic study of enclaves and their granitoid host-rocks. We define the types and relative abundance of the enclaves present, document their mineralogical and textural features in relation to the granites and associated mafic volcanic rocks of the region, propose a model for their origin, and discuss their implications for the genesis of the batholith. Our results clarify several longstanding misconceptions concerning the origin of enclaves and their bearing on the genesis and crystallization history of the batholith, and suggest a connection between mafic magmatism and batholith formation.

Geological setting

The Cornubian batholith is one of many post-orogenic granitic massifs emplaced during the late stages of the Carboniferous-Permian Hercynian orogeny (Exley and Stone, 1982). Exposures comprise six major plutons and numerous satellite bodies (Fig. 1) that extend over an area of about 10,000 km^2, and to a depth of ~ 10–12 km (Stone and Exley, 1986; Willis-Richards and Jackson, 1989). The dominant rock-type of the batholith is coarse-grained biotite muscovite granite (Exley and Stone, 1982), but fine-grained biotite granite, and Li-mica- and fluorite-bearing leucogranites are also represented (Stone, 1992). The biotite granites are strongly peraluminous (ASI ~ 1.17 to 1.28), and exhibit high K/Na, U, B, F, and $^{87}Sr/^{86}Sr$ ratios (0.710–0.716), and low Fe_2O_3/FeO (Exley and Stone, 1982; Darbyshire and Shepherd, 1985). These characteristics are broadly consistent with an S-type classification (see Chappell and White, 1992, and references therein), and there is a consensus in the recent literature that the coarse-grained biotite granites were generated by partial melting of pelitic rocks in the lower or intermediate crust (Stone and Exley, 1986; Charoy, 1986), and modified by crystal fractionation at the level of emplacement (Charoy, 1986; Ward *et al.*, 1992).

Recent studies have shown that, despite a relatively narrow compositional range, individual plutons record complex and protracted emplacement and cooling histories (e.g. Willis-Richards and Jackson, 1989; Chesley *et al.*, 1993; Chen *et al.*, 1993; Clark *et al.*, 1993). The batholithic rocks range in age from ~ 274 to 293 Ma (Chen *et al.*, 1993; Clark *et al.*, 1993) and intruded sub-greenschist to lower greenschist-grade metamorphic rocks of Devonian and Carboniferous age at shallow crustal levels (Robson, 1964; Floyd, 1971; Bromley, 1989). Late-stage hydrothermal processes have resulted in extensive kaolinization, greisenization, tourmalinization and Sn, Cu, W, As and Zn vein mineralization in and around the batholith.

Scattered remnants of the basaltic to strongly potassic Exeter volcanics are present at or near the base of the Permian Lower Sandstone and Breccia Group in Devon (Ussher, 1902; Knill, 1969, 1982). From their stratigraphic position and a K-Ar age of

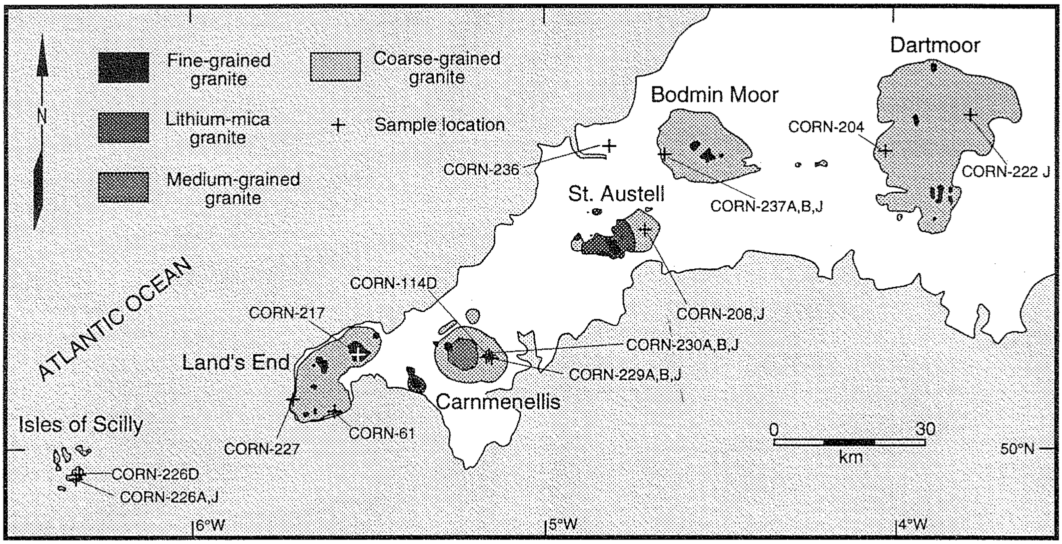

FIG. 1. Sample location map showing the major plutons and lithologies of the Cornubian batholith, southwest England (geology modified from Dangerfield and Hawkes, 1981). See Appendix I for sample descriptions.

TABLE 1. Previous interpretations of enclave origin, Cornubian batholith

Pluton	[1]Age (Ma)	Enclave type	Reference
Dartmoor (DM)	281–285	Basic igneous xenoliths	Reid *et al.*, 1912
		Basic igneous xenoliths Shale xenoliths	Brammall and Harwood, 1932
		Shale xenoliths	Lister, 1984
Bodmin Moor (BM)	281	Shale xenoliths	Ghosh, 1928; Lister, 1984
St. Austell (SA)	281	Shale xenoliths	Lister, 1984
Carnmenellis (CM)	293	Shale xenoliths	Ghosh, 1934; Al-Turki, 1972; Lister, 1984
		Restite	Jefferies, 1985; Charoy, 1986
Land's End (LE)	275	Shale xenoliths	Lister, 1984
Isles of Scilly (SI)	290	Igneous xenoliths	Osman, 1928;
		[2]'Type A granite'	Stone and Exley, 1989

[1] Ages based on monazite U/Pb dates for samples listed in Appendix I (Chen *et al.*, 1993).
[2] 'Type A granite' refers to xenoliths interpreted as earlier-emplaced, tonalitic to granodioritic rocks, disrupted by intrusion of the main-stage coarse-grained biotite granites (Exley and Stone, 1982; Stone and Exley, 1989).

291 $\pm$ 6 Ma (Miller *et al.*, 1962; Thorpe *et al.*, 1986), these volcanic rocks are in part coeval with the batholith. This is in accord with detailed textural studies by Tidmarsh (1932), who concluded that some of these volcanic rocks resulted from mixing of mafic and silicic magmas. Related WSW–ENE-trending lamprophryic dykes and sills cut the grain of metamorphic fabrics in southwest England (Exley and Stone, 1982), but do not intrude the granites or their contact aureoles.

Previous work on Cornubian enclaves

Several investigators have advocated a single origin for all enclaves in the Cornubian batholith (e.g. Ghosh, 1928, 1934; Lister, 1984; Jefferies, 1985), whereas others have distinguished 'shale xenoliths' from 'igneous xenoliths' (see Table 1 for summary). Shale xenoliths have generally been interpreted as either restite from the source region of magma generation (Exley and Stone, 1982; Jefferies, 1985; Charoy, 1986), or fragments of country-rock from the present level of exposure (Ghosh, 1928, 1934; Lister, 1984; Bromley, 1989), whereas igneous xenoliths have been regarded as either fragments of earlier-emplaced mafic-to-intermediate plutons (Brammall and Harwood, 1932), or xenoliths of country-rock that have been extensively modified by interaction with the granitic magma (Lister, 1984). In the most comprehensive study of enclaves to date, Brammall and Harwood (1932) concluded that igneous xenoliths are fragments of older diabasic, granodioritic and tonalitic rocks representing the initial stage of batholith development, and this interpretation has been adopted in subsequent summaries (Exley and Stone, 1964, 1982; Stone and Exley, 1989). Brammall and Harwood (1932) regarded shale xenoliths as fragments of metasedimentary material from depth.

Field and petrographic observations

Granitic rocks

The Cornubian batholith has been described in numerous studies since the early 1800's (De La Beche, 1839; Brammall and Harwood, 1932; Hall, 1974; Exley and Stone, 1982; Darbyshire and Shepherd, 1985; Charoy, 1986; Stone and Exley, 1986; Stone, 1992; and Ward *et al.*, 1992). We sampled mainly coarse-grained biotite granites from the major plutons, with an emphasis on enclave-bearing localities (see Fig. 1 and Appendix I). Several fine-grained biotite granites similar in appearance to the most silicic microgranular enclaves were also sampled for comparison. The biotite granites exhibit a restricted range in modal mineralogy (Fig. 2 and Table 2); in addition to feldspar and quartz, they contain biotite, muscovite, cordierite, andalusite and tourmaline. Cordierite,

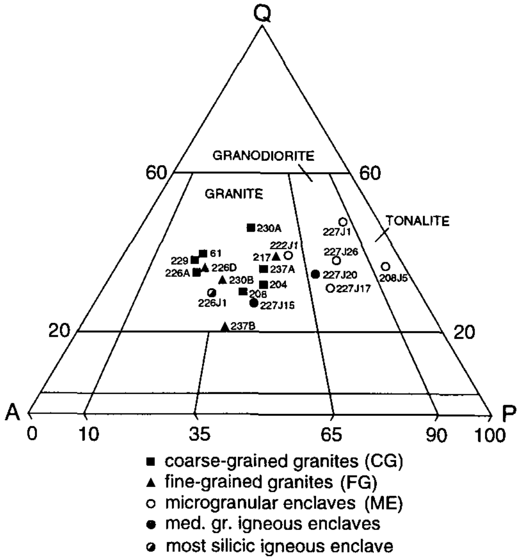

FIG. 2. Modal compositions of Cornubian granites and igneous enclaves on the IUGS triangle (Q — quartz, A — alkali feldspar, P — plagioclase). Data from point and grid counts of thin sections and stained slabs respectively.

muscovite and andalusite are restricted to layered enclaves and their disaggregation products in some granite samples, but may represent phenocrysts in others (e.g. samples 61, 217 and 229 in Table 2). Muscovite and andalusite are more abundant (muscovite ≈ biotite), and clearly phenocrystic, in the majority of fine-grained granites (e.g. 226A and 237A). As observed in other studies (e.g. Didier, 1973; Barbarin, 1991; Orsini *et al.*, 1991), there is a correlation between the types and abundance of enclaves and the chemistry and mineralogy of the host plutons. Plutons with muscovite ≈ biotite (e.g. Carnmenellis and Bodmin Moor) have a higher proportion of layered, aluminosilicate-bearing enclaves and higher ASI (~ 1.25 to 1.28), whereas those plutons with biotite > muscovite (e.g. Dartmoor and St. Austell) exhibit a higher proportion of microgranular enclaves and lower ASI (~ 1.17 to 1.18).

Enclave types and distribution

The broadest division of enclaves in the Cornubian granites is between those with igneous and those with non-igneous textures and mineralogies. Of the igneous variety, enclaves with microgranular texture are most common, and will be the focus of our discussion. We will employ the term 'microgranular enclave' (ME) for these enclaves, and the term 'non-igneous enclave' (NIE) for enclaves characterized by compositional layering and metamorphic mineral assemblages, including aluminosilicates. We will argue below that ME are the product of magma mixing, whereas NIE represent the residuum of metasedimentary material. Enclaves of both types are sparsely distributed in coarse-grained biotite granites, averaging much less than 1 vol.% of outcrops, and are virtually absent in fine-grained biotite- and Li-mica-bearing granites. NIE are most common overall, but rarely exceed 2 vol.% abundance. However, if one also considers minerals plausibly derived from disaggregation of NIE, then their total contribution may reach 5 vol.% in the Carnmenellis pluton. ME occur sparsely (< 1 vol.%) in all of the major plutons except Carnmenellis, being most abundant in the Dartmoor (Reid *et al.*, 1912; Brammall and Harwood, 1932), Land's End, and St. Austell plutons (Table 1). ME also occur in rare swarms, where their abundance is locally much higher (e.g. Birch Tor, Dartmoor granite). Hornfelsic xenoliths identifiable as country-rock are locally abundant near contacts (e.g. Porthmeor Cove, Land's End granite), but are otherwise rare to absent.

Microgranular enclaves. Enclaves that have been referred to as microgranular (Didier, 1973) or microgranitoid (Vernon, 1983) are common in granitic rocks worldwide, but are more abundant in I-type than in S-type granitoids (see discussions by Didier, 1973; Vernon, 1983, 1990; and papers in Didier and Barbarin, 1991*a*). With the exception of three samples, all enclaves with igneous compositions sampled in this study have microgranular texture, lack reaction rims, and are more mafic than their host rocks. The exceptions are samples 227J15 and 227J17 which are relatively silicic and medium-grained, and sample 226J1, which is nearly as silicic as its host granite but much finer-grained. These samples have a different origin than ME, and will be discussed separately. Rare composite ME consisting of a darker core in a paler matrix are also present as discussed below.

ME are typically elongate (2–45 cm in long dimension) with rounded, embayed, or crenulate margins (cf. Brammall and Harwood, 1932), and consist dominantly of fine-grained laths of biotite and plagioclase, with minor quartz, ilmenite, K-feldspar, and rare pinite after cordierite (Table 2 and Fig. 3A,B,C, and D). They also contain coarse-grained K-feldspar, sodic plagioclase, biotite and quartz, which are similar in texture and composition to phenocrysts in the host granite (Fig. 3A and B). These coarse-grained crystals and early-formed groundmass plagioclase and biotite are commonly poikilitically enclosed by aggregates of quartz or K-feldspar (Fig. 3C). K-feldspar megacrysts within

TABLE 2. Modal data for granite and enclave samples from the Cornubian batholith

Sample	PL	KF	QTZ	BT	ILM	CRD	AND	SIL	MS	TM	CRN	SP
61(CG)	15	37	34	7	1	3P	–	–	2	1	–	–
204(CG)	31	31	28	7	<1	<1	–	–	1	1	–	–
208(CG)	26	34	26	10	1	2	<1	–	1	<1	–	–
226A(CG)	15	40	30	7	1	2	–	–	3P	2	–	–
229(CG)	14	45	29	5	<1	1	1	–	5P	–	–	–
230A(CG)	21	25	39	8	1	2	1	–	3P	<1	–	–
237A(CG)	28	28	32	7	<1	<1	<1	–	5P	<1	–	–
217(FG)	29	24	34	2	<1	2P	2	–	4p	3	–	–
226D(FG)	17	41	31	5	<1	<1	<1	–	4p	<1	–	–
230B(FG)	21	39	29	3	<1	3	1	–	3p	1	–	–
237B(FG)	27	43	18	6	<1	–	2	–	3p	–	–	–
208J5(ME)	45	42	72	2	2	–	–	–	–	–	–	–
222J1(ME)	28	19	31	20	2	–	–	–	–	–	–	–
226J1(ME)	20	40	25	12	1	–	–	–	2	–	–	–
227J1(ME)	30	5	32	26	<1	5	–	–	2	–	–	–
227J15(ME)	25	27	20	20	3	2	–	–	5	<1	–	–
227J17(ME)	38	15	23	18	2	–	–	–	<1	–	–	–
227J20(ME)	36	17	27	20	2	–	–	–	–	–	–	–
227J26(ME)	32	12	25	28	1	–	–	–	–	–	–	–
237J2(ME)	39	5	26	28	2	–	–	–	<1	–	–	–
208J2(NIE)	18	–	25	25	2	28	–	2	–	–	tr	tr
208J8(NIE)	25	–	10	35	4	15	–	5	<1	–	<1	1
114D(NIE)	12	–	15	40	<1	5	25P	–	–	<1	–	–
229J2(NIE)	5	2	8	36	2	10	30P	–	6	–	–	–
230J1(NIE)	25	–	10	25	5	10	15P	–	3	15	–	–
230J2(NIE)	10	–	35	20	2	10	5P	–	4	15	–	–
237J1(NIE)	20	18	20	22	<2	–	5P	3f	10	<1	–	–

Abbreviations: (CG), coarse-grained granite; (FG), fine-grained granite; (ME) microgranular enclave; (NIE) non-igneous enclave; PL, plagioclase; KF, K-feldspar; QTZ, quartz; BT, biotite; ILM, ilmenite; CRD, cordierite; AND, andalusite; SIL, sillimanite; MS, muscovite; TM, tourmaline; CRN, corundum; SP, hercynitic spinel; P, large crystal-phenocryst in granite or porphyroblast in NIE; p, euhedral to subhedral groundmass crystals which appear primary in fine-grained granite; f, fibrolite; tr, trace; – not observed in thin section. Granites and enclaves contain traces of zircon, apatite and monazite at trace abundances.

some enclaves also show a crude alignment suggestive of magmatic flow (Fig. 3A), and some are mantled by plagioclase (Fig. 3E). Accessory apatite, zircon, monazite, pyrrhotite and an Fe–Cu sulphide are typically associated with biotite, or present as inclusions in late-formed quartz (Fig. 3F). Hornblende-bearing enclaves have been recorded from the Dartmoor granite (Brammall and Harwood, 1932), but were not observed in this study, and must be very rare.

Non-igneous enclaves. In southwest England enclaves with non-igneous fabric and mineralogy have been referred to mainly as 'shale xenoliths' (Ghosh, 1928, 1934; Brammall and Harwood, 1932; Al-Turki, 1972; Lister, 1984). Similar enclaves have been described elsewhere as metamorphic, surmicaceous, restitic, schistose, gneissic or hornfelsic (Didier, 1973; Chappell *et al.*, 1987; papers in Didier and Barbarin, 1991*a*). Most NIE in Cornubian granites display compositional layering parallel to their long dimension, but rarely exhibit a true mineral foliation (Fig. 4A). A few such enclaves lack layering, and have a granoblastic texture. NIE consist dominantly of biotite, aluminosilicates, plagioclase, cordierite and quartz, but some also contain muscovite, hercynite, corundum, and ilmenite (see Table 2 and Fig. 4B,C and D). Some NIE contain a mineral assemblage dominated by andalusite-biotite(-muscovite) whereas others contain sillimanite- and biotite-rich assemblages. Accessory minerals include apatite, zircon, monazite, pyrrhotite and an Fe–Cu sulphide. Most NIE have reaction rims rich in biotite, tourmaline or cordierite, and some larger examples contain

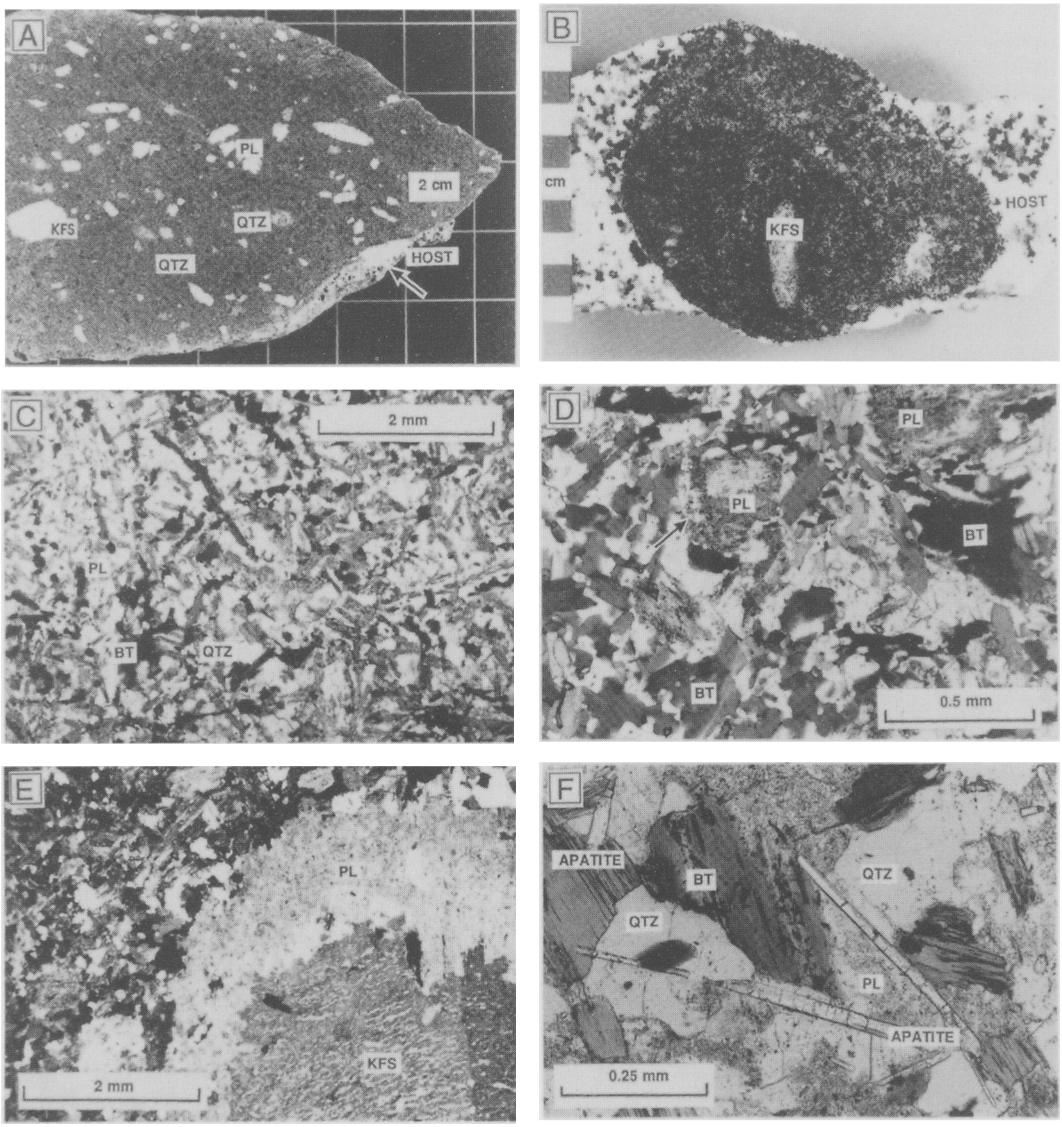

FIG. 3. Microgranular enclaves (ME) in hand-specimen and thin section (mineral abbreviations as in Table 2). (A) Large ME (222J1) from the Dartmoor granite containing large crystals of K-feldspar, plagioclase, biotite and quartz set in a fine-grained groundmass consisting dominantly of plagioclase, biotite and quartz (scale bar = 2 cm). Host granite is seen at lower-right (arrow). (B) Composite ME (208J5) from the St. Austell granite (mineralogy as in 3A). The darker portion of enclave is finer-grained and contains more biotite and less quartz than the paler (scale bar in centimetres). (C) Photomicrograph (plane-polarized light) of a ME from the St. Austell granite (207J3) with fine-grained, bladed texture. Elongate crystals of plagioclase (turbid due to sericitization) and biotite (dark) are surrounded by smaller and more equant crystals of quartz (clear). (D) Photomicrograph (plane-polarized light) of partially sericitized plagioclase (arrow) and biotite phenocrysts set in the finer-grained groundmass of an enclave from the Dartmoor granite (222J1). (E) Photomicrograph (crossed nicols) of a K-feldspar megacryst within a ME from the Lands End granite (227J26). The megacryst is rounded and mantled by partially sericitized plagioclase. (F) Photomicrograph (plane-polarized light) of apatite needles in a ME from the St. Austell granite (207J1). Apatite in ME is generally elongate, suggesting undercooled crystallization.

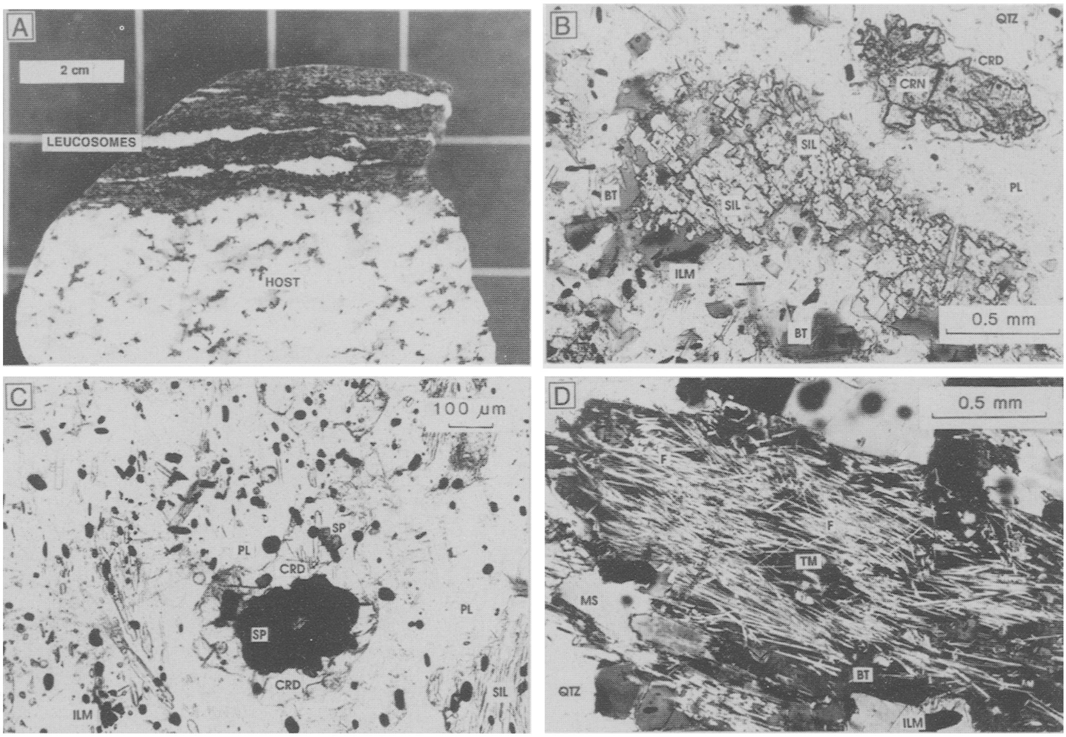

FIG. 4. Non-igneous enclaves (NIE) in hand-sample and thin section (mineral abbreviations as in Table 2). (A) Portion of an unusually large NIE with prominent layering (237J1) from the Bodmin Moor granite. The dark portions of the enclave consist mainly of biotite, plagioclase and andalusite, with lesser quartz, muscovite and K-feldspar. The lighter laminae, interpreted as leucosomes, consist primarily of K-feldspar, sodic plagioclase and quartz (scale bar = 2 cm). (B) Photomicrograph (plane-polarized light) of an enclave (208J2) from the St. Austell granite displaying coarse-grained sillimanite rimmed by biotite, and corundum rimmed by cordierite. (C) Photomicrograph (plane-polarized light) of an enclave (208J8) from the St. Austell granite containing domains of hercynitic spinel and sillimanite enclosed in cordierite. Sample also contains abundant ilmenite and Fe-Cu sulphides. (D) Photomicrograph (crossed nicols) of NIE (114D) from the Carnmenellis pluton with locally abundant fibrolite and fine-grained sillimanite as inclusions in tourmaline, biotite and muscovite. Sample also contains andalusite porphyroblasts which show little or no reaction to sillimanite.

leucosomes (generally elongated parallel to layering) consisting mainly of feldspar and quartz (Fig. 4A). NIE lack the large crystals of K-feldspar, sodic plagioclase and quartz that are common in ME.

Mineral textures and compositions

Plagioclase and K-feldspar. Plagioclase phenocrysts and inclusions in both the coarse-grained and fine-grained granites range in composition from albite to andesine, but the most calcic compositions are commonly altered to sericite (Table 3, Fig. 5A and B). Normal zoning is typical, with crystal cores averaging An_{30}, and crystal rims ranging to near end-member albite (cf. Ward *et al.*, 1992). Plagioclase in ME ranges in composition from albite to labradorite (Fig. 5C), with large crystals intergrown with green biotite exhibiting the most calcic compositions. The rims of these large crystals range from An_{22} to An_{37}, whereas the few cores that have escaped sericitization range from An_{36} to An_{59} (Fig. 3D). Normally zoned plagioclase microphenocrysts in ME range from An_7 to An_{34} (averaging An_{28}), but nearly complete replacement of crystal cores by sericite biases analyses toward sodic compositions. Rapakivi-type mantles on K-feldspar in ME range from An_4 to An_{28} (Fig. 5C). Plagioclase in the groundmass of NIE ranges from An_5 to An_{44} (Fig. 5E), with the most calcic compositions occurring in enclaves with the highest metamorphic grades and Al_2O_3 contents (e.g.

TABLE 3. Representative electron microprobe analyses of feldspar from granites and enclaves

	CG/BM 237 KF M	CG/SA 208 PL P R	CG/SA 208 PL P C	FG/BM 237B PL(m)C	FG/CM 230B KF (m)	FG/BM 237B PL(m)	ME/DM 222J1 PL(MP)C	ME/DM 222J1 KF M(SP)	ME/SA 208J5B PL(MP)C	ME/SA 208J5B PL(SP)
Wt.% oxide										
SiO_2	64.84	65.26	61.92	59.92	65.31	63.27	53.61	64.97	57.21	62.20
Al_2O_3	18.62	22.13	24.37	25.47	19.00	23.22	29.50	18.46	27.21	23.97
Fe_2O_3	0.00	0.02	0.01	0.03	0.04	0.02	0.14	0.03	0.12	0.00
CaO	0.06	3.17	5.82	6.22	0.06	3.80	11.71	0.09	9.33	5.19
SrO	0.15	0.03	0.03	0.16	0.15	0.00	0.05	0.20	0.05	0.11
BaO	0.07	0.03	0.03	0.11	0.32	0.02	0.01	0.22	0.00	0.00
Na_2O	1.43	9.68	8.39	8.19	2.48	9.56	5.16	1.03	6.48	8.85
K_2O	14.73	0.47	0.25	0.25	13.31	0.26	0.16	15.38	0.29	0.20
Total	99.90	100.79	100.83	100.34	100.67	100.13	100.35	100.37	100.69	100.51
IV	4.000	3.998	3.996	4.003	4.001	4.004	3.994	3.995	3.991	3.995
VI	1.002	0.998	1.008	1.023	1.007	1.013	1.029	1.009	1.025	1.017
Sum	5.002	4.996	5.003	5.026	5.008	5.017	5.023	5.004	5.016	5.013
Ab	0.13	0.82	0.71	0.69	0.22	0.81	0.44	0.09	0.55	0.75
An	0.00	0.15	0.27	0.29	0.00	0.18	0.55	0.00	0.44	0.24
Or	0.87	0.03	0.01	0.01	0.78	0.01	0.01	0.90	0.02	0.01

	ME/LE 227J1 PL(RAP)R	ME/LE 227J26 PL(m)	L 236 KF P C	L 236 KF m	NIE/SA 208J8 PL	NIE/SA 229J PL(G)	NIE/BM 2237J1 PL NR SP	NIE/BM 237J1 KF	NIE/BM 237J1 KF(L)	NIE/L/BM 237J1 PL(L)
Wt.% oxide										
SiO_2	62.28	63.35	64.19	64.26	58.14	56.00	67.81	65.02	65.39	65.49
Al_2O_3	24.39	23.17	18.60	18.09	26.43	27.68	20.42	18.71	18.27	21.63
Fe_2O_3	0.01	0.05	0.56	0.52	0.15	0.07	0.01	0.01	0.00	0.00
CaO	5.79	4.05	0.10	0.19	8.34	9.31	1.16	0.05	0.02	2.65
SrO	0.01	0.03	0.39	0.34	0.05	0.03	0.07	0.16	0.18	0.06
BaO	0.02	0.00	0.38	0.07	0.02	0.01	0.00	0.10	0.00	0.00
Na_2O	8.52	9.37	1.96	2.19	7.13	6.48	11.28	1.45	0.83	10.17
K_2O	0.51	0.41	13.65	13.41	0.13	0.13	0.13	14.77	15.86	0.14
Total	101.54	100.44	99.84	99.07	100.38	99.71	100.88	100.27	100.56	100.13
IV	3.990	3.999	4.001	3.994	3.992	3.999	3.994	4.000	3.993	3.998
VI	1.026	1.016	1.003	1.012	1.025	1.025	1.014	1.003	1.010	1.000
Sum	5.016	5.015	5.005	5.006	5.018	5.025	5.008	5.004	5.003	4.999
Ab	0.71	0.79	0.18	0.20	0.60	0.55	0.94	0.13	0.07	0.87
An	0.27	0.19	0.01	0.01	0.39	0.44	0.05	0.00	0.00	0.12
Or	0.03	0.02	0.82	0.79	0.01	0.01	0.01	0.87	0.93	0.01

Abbreviations: P, phenocryst; SP, phenocryst derived from the host granite; MP, phenocryst derived from the mafic end-member; C, core; R, rim; L, minerals in enclave leucosomes; m, microphenocryst; M, megacryst; RAP, rapakivi rim; NR, near; G; groundmass. Other abbreviations same as in Table 2 and Appendix I.
Cations per 8 oxygens

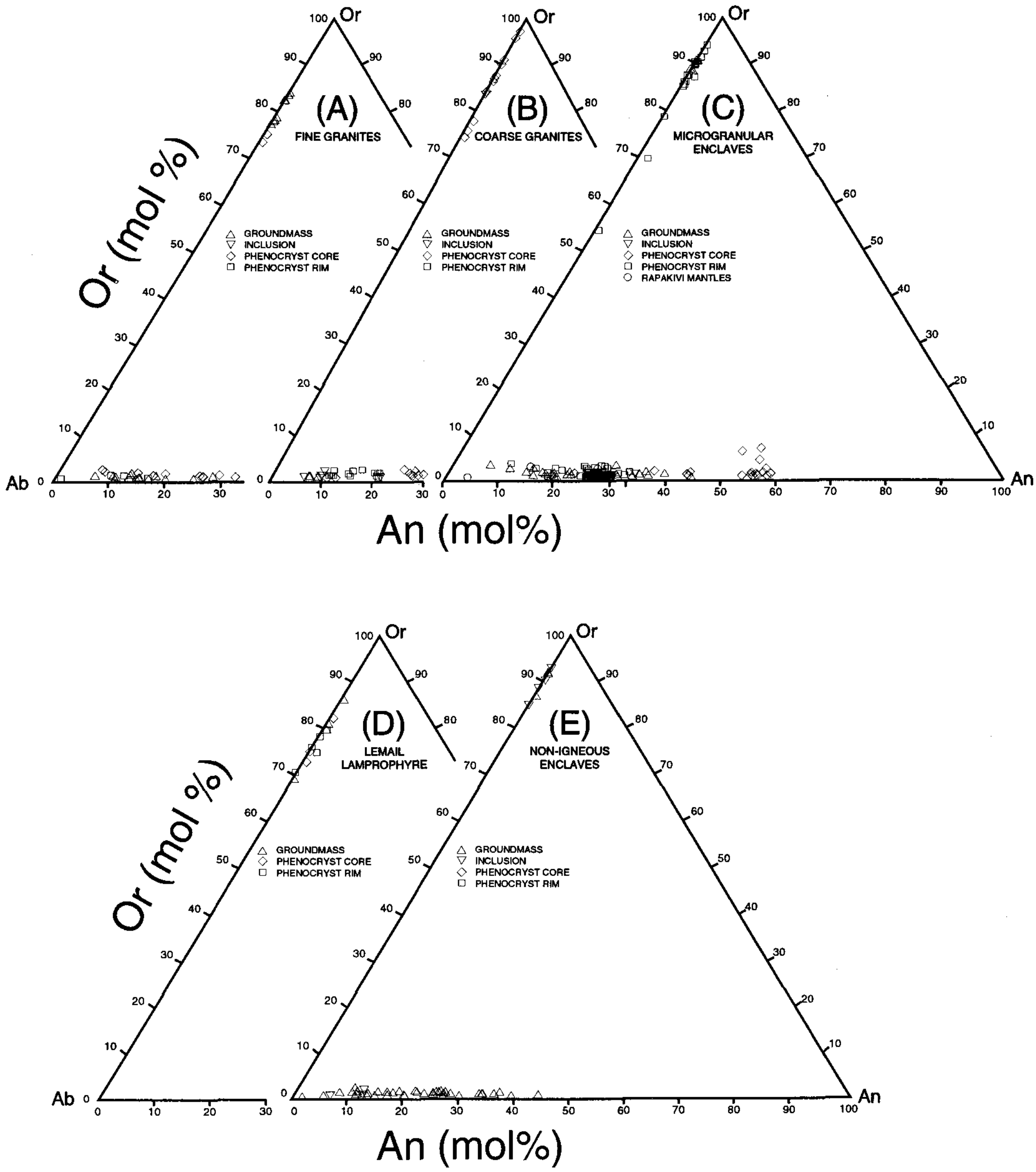

FIG. 5. Feldspar compositions in granites, enclaves and Lemail lamprophyre. (A) Fine-grained granites, (B) Coarse-grained granites, (C) Microgranular enclaves, (D) Lemail lamprophyre, and (E) Non-igneous enclaves. See Table 3 for representative data.

208J8). Conversely, the most sodic compositions (An_{2-10}) are restricted to lower-grade NIE containing K-feldspar, muscovite and andalusite (e.g., 237J1), and leucosomes in these enclaves.

K-feldspar is present in the granites both as groundmass crystals and megacrysts up to several cm in long dimension. Microscopically clear regions of megacrysts and groundmass grains in granites have compositions in the range Or_{74} to Or_{97} (Fig. 5A and B). K-feldspar ranging from Or_{69} to Or_{92} is present in the groundmass of ME where it poikilitically encloses plagioclase and biotite micro-

TABLE 4. Representative electron microprobe analyses of biotite from granites and enclaves

	CG/BM 237A P	CG/CM 230 P	CG/SA 208 P	FG/BM 237B P C	IE/BM 237J2 m	ME/DM 222J1 m	ME/DM 222J1 MP	ME/DM 222J1 SP R	LAM 236 P C	NIE/CM 229J2 m	NIE/CM 230J2 m	NIE/SA 208J8 m
Wt.% oxide												
SiO_2	35.00	35.84	36.46	35.64	35.11	35.41	37.16	36.16	37.73	35.90	35.43	34.78
TiO_2	2.81	2.36	1.91	2.88	3.30	3.87	0.97	3.66	5.68	1.48	2.16	2.04
Al_2O_3	20.36	21.24	20.82	19.56	18.98	15.03	15.02	15.20	13.03	20.17	20.77	19.42
Cr_2O_3	0.02	0.04	0.03	0.04	0.07	0.03	0.13	0.04	0.36	0.05	0.05	0.12
FeO	23.50	22.34	19.80	21.58	24.86	23.23	18.76	23.42	5.68	19.15	23.48	21.90
MnO	0.53	0.26	0.27	0.18	0.31	0.58	0.43	0.59	0.11	0.29	0.18	0.32
MgO	4.05	4.68	6.05	7.12	5.69	8.39	12.57	8.24	20.18	8.85	4.90	7.37
CaO	0.00	0.00	0.00	0.00	0.04	0.04	0.01	0.02	1.47	0.01	0.00	0.02
BaO	0.05	0.10	0.10	0.17	0.11	0.32	0.07	0.21	1.40	0.07	0.10	0.09
Na_2O	0.08	0.16	0.21	0.20	0.20	0.07	0.12	0.10	0.17	0.18	0.22	0.32
K_2O	9.61	9.25	9.41	9.73	9.46	9.14	9.38	9.46	9.22	9.26	9.27	9.13
Total	96.01	96.27	95.06	97.1	98.13	96.11	94.62	97.1	95.03	95.41	96.56	95.51
Si-	2.699	2.723	2.772	2.694	2.670	2.748	2.851	2.775	2.756	2.717	2.703	2.678
Ti-	0.163	0.135	0.109	0.164	0.189	0.226	0.056	0.211	0.312	0.084	0.124	0.118
Al-	1.851	1.902	1.865	1.743	1.701	1.374	1.358	1.374	1.122	1.800	1.868	1.763
Cr-	0.001	0.003	0.002	0.002	0.004	0.002	0.008	0.002	0.021	0.003	0.003	0.007
Fe-	1.516	1.419	1.259	1.364	1.581	1.508	1.204	1.503	0.347	1.213	1.499	1.410
Mn-	0.034	0.017	0.017	0.011	0.020	0.038	0.028	0.038	0.007	0.019	0.012	0.021
Mg-	0.466	0.530	0.685	0.803	0.645	0.971	1.437	0.943	2.198	0.999	0.558	0.846
K-	0.946	0.897	0.913	0.939	0.918	0.905	0.918	0.927	0.859	0.894	0.903	0.897
Ba-	0.002	0.003	0.003	0.005	0.003	0.010	0.002	0.006	0.040	0.002	0.003	0.003
Ca-	0.000	0.000	0.000	0.000	0.003	0.003	0.001	0.002	0.115	0.000	0.000	0.002
Na-	0.012	0.023	0.030	0.029	0.029	0.010	0.017	0.014	0.023	0.026	0.032	0.047
Al VI	0.55	0.62	0.64	0.44	0.37	0.12	0.21	0.15	0.00	0.52	0.57	0.44
Mg#	0.23	0.27	0.35	0.37	0.29	0.39	0.54	0.39	0.86	0.45	0.27	0.38

Mineral, rock type, and pluton abbreviations same as in Table 2 and Appendix I.
Cations based on 11 oxygens.

phenocrysts, or surrounds large anhedral quartz grains. K-feldspar megacryst compositions (Or_{78-90}) in ME overlap with those of phenocrysts in the host granites (Fig. 5A–C). K-feldspar is rare in NIE, occurring only in the groundmass of some low-grade enclaves (Or_{86-91}) and in leucosomes (Or_{84-91}). K-feldspar in the Lemail lamprophyre dyke (sample 236) ranges from Or_{69} to Or_{86} (Fig. 5D), but can be differentiated from K-feldspar in granites and enclaves by its higher BaO and SrO concentrations (Table 3).

Biotite and muscovite. Biotite in granites and enclaves is foxy-red, with inclusions of ilmenite, apatite, zircon and monazite. That in microgranular enclaves overlaps in composition with that in granites, but is generally lower in Al^{VI}, and extends to more Mg-rich compositions (Table 4 and Fig. 6). Rare Mg-rich greenish biotite associated with labradorite in some ME (Fig. 3D) is lower in Al^{VI} and Ti, and higher in Mg than other analysed grains, but biotite from the two most aluminous metamorphic enclaves studied is also relatively low in Ti and high in Mg. Phlogopite from the Lemail lamprophyre is much higher in Mg and Ti, and lower in Al^{VI} than the most Mg-rich biotite in ME.

Muscovite is present in granites, some NIE, and a few igneous enclaves. Most commonly, it forms anhedral-to-subhedral masses mantling and replacing andalusite or cordierite, or veinlets cutting K-feldspar and plagioclase. More rarely, muscovite occurs as coarse, subhedral-to-euhedral books associated with biotite in coarse-grained granites (e.g. 226A, 229, 230A), or as subhedral groundmass crystals in fine-grained granites (e.g. 217, 226D, and 230B), indicating a primary origin in these rocks (Table 2). Coarse-grained muscovite is present in some NIE from the Carnmenellis, Isles of Scilly, and Bodmin Moor plutons, but is absent in ME, which contain only fine-grained, clearly secondary grains. The three igneous enclaves distinct from ME (226J1, 227J15, and 227J17) mentioned earlier also contain sparse coarse-grained muscovite (Table 2).

Cordierite occurs as anhedral-to-euhedral grains in the granitic rocks, and as irregular masses in both ME and NIE. In NIE it is present: (1) as fine-grained intergrowths with quartz, (2) enclosing sillimanite, corundum and hercynitic spinel (e.g. Fig. 4C), (3) in melasomes with biotite, and (4) as multi-grain aggregates at granite-enclave contacts. Cordierite compositions in granitic rocks and NIE are both Fe-rich, with molar Mg/[Mg+Fe] ranging from 0.29 to 0.56 (Table 5), but some anhedral grains in granites and NIE range to higher MnO concentrations than subhedral grains in granites.

The cordierite is deficient in octahedrally coordinated cations (i.e. low Fe+Mg+Mn), with Na in channelways maintaining stoichiometry (Table 5).

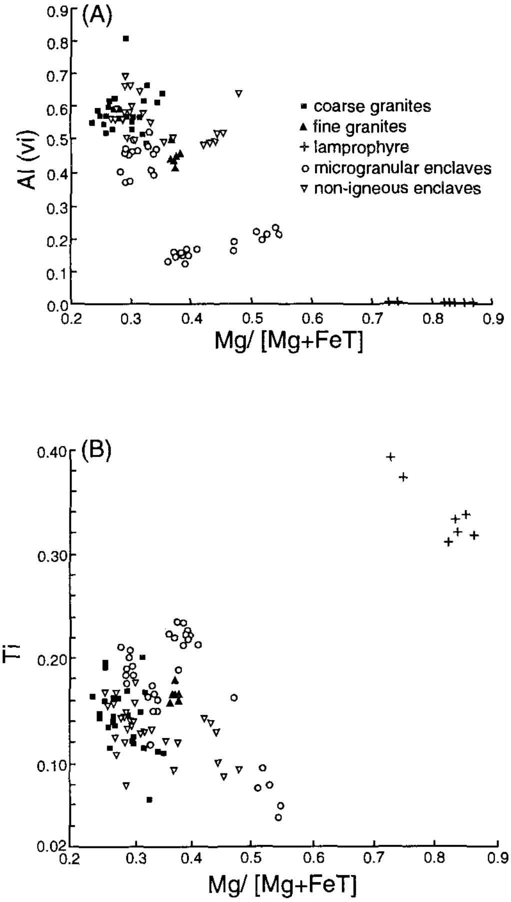

FIG. 6. Biotite compositions in granites, enclaves and Lemail lamprophyre. (A) Al^{VI} *vs* Mg/[Mg+Fe], (B) Ti *vs* Mg/[Mg+Fe]. See Table 4 for representative data.

Na_2O contents in the analysed samples range from ~ 0.3 to 1.6 wt.%. Assuming that low totals are due to the presence of volatiles, the concentration of such elements ranges from ~ 2 to 6 wt.%, but the filled tetrahedral sites and high Na contents suggest that some other cation (possibly Li or Be) must be present to maintain charge balance. Cordierite in many of the granite samples and in all ME is replaced by pinite.

Spinels, aluminosilicates and corundum. Hercynitic spinel (molar Fe/[Fe+Mg] = 0.91 to 0.93) is common in NIE (Table 6). It typically forms small, euhedral-to-subhedral grains enclosed in cordierite and associated with sillimanite and ilmenite (Fig. 4C). Chromite is present as rare inclusions in other minerals in some silica-deficient, high-grade NIE (e.g. 208J8). Aluminosilicates and/or corundum are present in all NIE (Table 6). Andalusite is more

TABLE 5. Representative electron microprobe analysis of cordierite in granites and enclaves

	CG/CM 230A	CG/LE 227J29	FG/CM 230B	NIE/CM 229J2	NIE/CM 230J2	NIE/SA 208J8	NIE/SA 208J8	NIE/SA 208J2
Wt.% oxide								
SiO_2	47.54	46.86	47.06	47.33	46.75	46.70	46.14	46.39
TiO_2	0.00	0.00	0.05	0.05	0.02	0.05	0.04	0.03
Al_2O_3	32.36	31.74	32.02	32.15	31.78	31.87	31.31	31.80
FeO	10.62	11.71	10.46	9.32	12.78	12.06	13.47	13.73
MnO	0.41	0.33	0.29	0.55	0.80	0.72	0.90	0.91
MgO	5.74	4.34	5.54	5.54	3.37	4.45	3.52	3.27
CaO	0.00	0.02	0.01	0.03	0.02	0.02	0.04	0.04
Na_2O	0.93	1.59	1.07	1.38	1.39	0.85	0.87	1.06
K_2O	0.00	0.01	0.00	0.00	0.00	0.00	0.00	0.00
H_2O	2.39	3.41	3.50	3.66	3.09	3.27	3.71	2.77
Total	97.61	96.59	96.50	96.34	96.91	96.73	96.29	97.23
Si-	5.005	5.022	5.009	5.027	5.024	5.003	5.007	4.993
Ti-	0.000	0.000	0.004	0.004	0.001	0.004	0.003	0.002
Al-	4.015	4.010	4.017	4.025	4.026	4.025	4.005	4.035
Fe-	0.935	1.049	0.932	0.827	1.149	1.080	1.223	1.236
Mn-	0.036	0.030	0.026	0.049	0.073	0.066	0.083	0.083
Mg-	0.901	0.693	0.880	0.878	0.541	0.711	0.569	0.525
K-	0.000	0.002	0.000	0.000	0.000	0.000	0.000	0.000
Ca-	0.000	0.002	0.001	0.003	0.002	0.003	0.004	0.004
Na-	0.191	0.330	0.222	0.285	0.289	0.176	0.184	0.222
Mg#	0.49	0.40	0.49	0.51	0.32	0.40	0.32	0.30
M+2	1.872	1.774	1.838	1.757	1.765	1.860	1.879	1.848
M+2,+1	2.063	2.106	2.059	2.042	2.054	2.036	2.063	2.069

Total Fe as FeO; H_2O by difference; cations based on 18 oxygens.
Abbreviations as in Table 2 and Appendix I.

common than sillimanite (except in enclaves from the St. Austell granite), comprising up to 30 vol.% of some samples (Table 2). It occurs as porphyroblasts several cm in length, and as anhedral groundmass grains. Pink pleochroic cores are relatively rich in Fe compared to clear rims (Table 6). Sillimanite (> 2 μm) is most abundant in enclaves from the St. Austell pluton (Fig. 4B and C). Fibrolite (< 2 μm) occurs as inclusions in biotite, muscovite and tourmaline in NIE from the Isles of Scilly and Carnmenellis plutons (Fig. 4D). These rocks also contain abundant andalusite porphyroblasts, which show little or no reaction to sillimanite, suggesting that andalusite persists metastably into the sillimanite field, and that initial sillimanite formation is due to a reaction other than the breakdown of andalusite (Pattison, 1992). Corundum forms anhedral masses surrounded by cordierite in several NIE collected from the St. Austell pluton (Fig. 4B).

Opaque minerals. Ilmenite is ubiquitous as inclusions and small grains in the granitic rocks and enclaves. It is particularly abundant in some NIE, comprising up to 5 vol.% of several samples (Fig. 4C and Table 6). Ilmenite contains a very low hematite component (< 0.03 mol.%), low MgO, and high MnO. Trace amounts of pyrrhotite and Fe–Cu sulphide occur in both NIE and ME, but were not analysed. Fine-grained, platy opaques, interpreted as graphite, are present as inclusions in other minerals in some NIE, especially from the St. Austell pluton.

Whole-rock chemistry

Whole-rock analyses of enclaves and granitic host-rocks are given in Table 7 and plotted in Figs. 7 and 8. Granitic to tonalitic ME generally extend the compositional trends of their host granites to more

TABLE 6. Representative electron microprobe analyses of spinel, ilmenite, and andalusite in granites and enclaves

	NIE/SA	NIE/SA	NIE/SA	NIE/SA	NIE/SA	NIE/SA	CG/LE	CG/SA	NIE/CM
		Spinel				Ilmenite			Andalusite
	208J8	208J8	208J2	208J8	208J1	208J1	61	208	114D
Wt.% oxide									
SiO_2	0.00	0.01	0.03	0.02	0.02	0.02	0.00	0.00	36.74
TiO_2	0.06	0.08	0.02	52.38	51.43	52.30	52.76	52.88	0.00
Al_2O_3	57.60	57.16	58.21	0.01	0.03	0.06	0.01	0.01	62.06
Cr_2O_3	0.39	1.03	0.59	0.00	0.05	0.02	0.00	0.01	0.02
FeO	36.31	36.61	33.90	41.60	42.89	44.79	41.14	45.42	0.20
MnO	0.61	0.67	0.53	5.04	5.11	2.48	6.32	2.15	0.03
MgO	1.87	1.50	1.38	0.06	0.08	0.07	0.04	0.07	0.00
ZnO	1.99	1.92	3.83	NA	NA	NA	NA	NA	NA
Total	98.83	98.99	98.52	99.11	99.62	99.75	100.27	100.57	99.05
Si-	0.000	0.000	0.001	0.001	0.001	0.000	0.000	0.000	1.000
Ti-	0.001	0.002	0.000	1.002	0.985	0.996	0.999	0.998	0.000
Al-	1.975	1.963	1.997	0.000	0.001	0.002	0.000	0.000	1.990
Cr-	0.009	0.024	0.014	0.000	0.001	0.000	0.000	0.000	0.000
Fe-	0.883	0.892	0.825	0.884	0.913	0.948	0.866	0.954	0.005
Mn-	0.015	0.017	0.013	0.109	0.110	0.053	0.135	0.046	0.001
Mg-	0.081	0.065	0.060	0.002	0.003	0.003	0.001	0.002	0.000
Zn-	0.043	0.041	0.082						
IV	1.985	1.989	2.012	1.002	0.986	0.996	0.999	0.998	3.990
VI	1.022	1.015	0.981	0.995	1.026	1.004	1.002	1.002	
XFe	0.92	0.93	0.93 Ilm	1.000	0.977	0.996	0.998	0.998	
XMg	0.08	0.07	0.07 Hem	0.000	0.023	0.004	0.002	0.002	

NA; not analysed. Total Fe as FeO.
Abbreviations as in Appendix I.

mafic compositions (Fig. 2 and Table 2), and can be distinguished from NIE by their lower Al_2O_3, MgO, and Cr, and higher SiO_2, CaO, P_2O_5, *REE*, Th and Sr contents. These chemical differences are consistent with the mineralogical and textural relationships summarized above. Three of the most felsic igneous enclaves (226J1, 227J15 and 227J17) are texturally and compositionally distinct from ME, and probably represent fragments of fine- and medium-grained granitic rocks incorporated in the coarse-grained host, as suggested by previous workers (Table 1). All other enclaves with igneous compositions and textures are typical 'mafic microgranular enclaves' (Didier and Barbarin, 1991*b*), which are widely accepted as forming by interaction of mafic and felsic magmas (Vernon, 1983, 1990; Didier and Barbarin, 1991*a*, and references therein).

Two of the largest ME are megascopically heterogeneous, allowing analyses of different portions of the same sample (Fig. 3A and B). Sample 208J5 is a composite enclave consisting of a melanocratic enclave (analysis 5B in Table 7) enclosed in a paler enclave (analysis 5A). Sample 222J1 contains abundant large crystals of K-feldspar, plagioclase, quartz and biotite; analysis 222J1A in Table 7 is of the whole-rock, whereas analysis 222J1B represents material that was hand-picked to exclude large crystals (i.e. a groundmass separate). Lines connecting these sample pairs trend parallel to the broader array defined by ME and the hosting granites for elements (e.g. Al, Fe, Mg, Cr) that typically show low mobility (Fig. 7).

Granites and ME define broadly linear trends for more immobile elements, with a gap between mafic ME and most felsic igneous enclaves (Fig. 7). Analyses of ME sampled by Brammall and Harwood (1932) extend the arrays defined by our ME samples to more basic compositions, where they overlap the broad field defined by the Cornubian lamprophyre dykes and the Exeter Volcanics (Fig. 8).

TABLE 7. Whole-rock chemical data for granites and enclaves

	Coarse granites							Fine granites			
	61	204	208	226A	229	230A	237A	217	226D	230B	237B
XRF (Wt.% oxide)											
SiO_2	71.89	73.59	72.68	72.29	72.56	72.59	72.71	72.73	72.87	73.95	72.51
TiO_2	0.37	0.28	0.31	0.24	0.22	0.29	0.20	0.16	0.16	0.11	0.31
Al_2O_3	14.30	13.54	14.18	15.20	14.99	14.68	14.89	14.65	14.90	14.78	14.76
Fe_2O_3T	2.67	2.45	2.24	1.75	1.72	2.02	1.57	1.40	1.39	1.18	1.58
MnO	0.05	0.05	0.06	0.03	0.04	0.05	0.04	0.03	0.02	0.06	0.02
MgO	0.62	0.38	0.40	0.36	0.40	0.42	0.30	0.26	0.24	0.18	0.37
CaO	0.79	0.68	0.94	0.76	0.74	1.05	0.78	0.70	0.66	0.74	1.03
Na_2O	2.65	2.99	2.92	2.88	2.88	3.24	3.24	3.41	2.71	3.70	3.18
K_2O	5.30	5.06	5.08	5.36	5.26	4.31	4.92	4.94	5.84	4.38	5.15
P_2O_5	0.29	0.23	0.26	0.25	0.23	0.27	0.26	0.29	0.20	0.22	0.22
Total	98.93	99.25	99.07	99.12	99.04	98.91	98.91	98.58	98.98	99.30	99.13
XRF (ppm)											
V	24	14	12	11	12	15	<7	<6	<6	<6	10
Cr	14	<6	<6	8	14	9	<6	<6	<6	7	<6
Ni	<6	<6	<6	<6	<6	<6	<6	<6	<6	<6	<6
Zn	42	42	24	29	51	21	46	21	27	18	54
Rb	395	481	425	464	459	403	408	528	398	300	265
Sr	86	52	75	102	92	90	88	59	92	72	170
Y	22	28	21	11	12	11	14	17	8	14	6
Zr	150	136	127	106	102	120	90	67	77	45	135
Nb	22	23	24	15	16	18	15	25	16	17	10
Ba	280	159	240	223	209	179	184	131	242	105	759
INA (ppm)											
Cl	440	280	<180	85	<140	<300	<400	440	174	<170	<110
Sc	4.9	4.6	4.2	2.8	3.0	3.7	2.4	3.6	2.3	2.4	2.0
V	24	11	14	14	15	13	<11	8	<6	<9	12
Cr	12	5	6	9	12	9	6	<4	<3	<4	4
Ga	21	30	<30	<50	31	<30	<40	<50	25	<30	22
Rb	439	471	433	456	499	394	399	540	396	288	255
Cs	27	49	28	25	37	51	27	50	25	30	9
Hf	4.9	4.5	3.8	3.2	3.7	3.9	2.7	2.3	2.8	1.6	4.6
Th	25.3	19.1	20.6	23.0	18.6	22.5	12.4	9.2	15.2	5.9	17.5
U	14.8	7.0	16.3	4.5	10.1	16.7	12.3	20.0	4.3	17.0	7.1
La	41	27	33	37	29	39	24	15	26	12	43
Ce	98	58	75	93	66	82	52	39	59	29	105
Nd	61	12	45	40	30	31	21	<10	13	7	51
Sm	8.1	5.6	6.4	6.7	4.6	6.9	4.0	2.9	4.7	2.1	6.8
Eu	0.86	0.56	0.75	0.72	0.71	0.65	0.64	0.45	0.54	0.41	0.93
Tb	0.6	0.72	<0.07	0.35	0.41	0.53	0.46	0.39	0.27	<0.03	0.55
Dy	4.5	4.9	3.0	2.4	1.9	<15	<23	2.3	1.9	1.9	1.1
Yb	2.9	3.4	3.6	<1.7	2.0	1.8	2.2	2.3	1.9	3.2	<0.9
Lu	0.23	0.21	0.24	<0.3	<0.3	0.12	<0.3	0.22	<0.25	<0.3	<0.03

	Microgranular enclaves										
	208J5A	208J5B	222J1A	222J1B	226J1	227J1	227J20	227J26	227J15	227J17	237J2
XRF (Wt.% oxide)											
SiO_2	64.79	63.34	65.72	64.64	70.64	68.15	65.64	62.48	65.41	65.56	62.92
TiO_2	1.08	1.20	0.92	1.04	0.35	0.62	1.06	1.33	1.10	0.9	1.38
Al_2O_3	15.61	15.67	15.63	15.40	15.07	15.49	15.37	15.54	14.74	16.11	14.49
Fe_2O_3T	6.60	7.44	5.67	6.26	2.31	5.01	5.96	8.01	6.32	5.32	8.9
MnO	0.12	0.13	0.11	0.12	0.03	0.07	0.07	0.09	0.08	0.7	0.11
MgO	1.44	1.62	1.80	2.03	0.51	1.29	1.46	2.29	1.41	1.16	1.97
CaO	2.61	2.58	2.49	2.53	0.70	1.75	2.02	2.11	1.52	161	2.63
Na_2O	3.69	3.52	3.65	3.61	2.72	3.60	3.84	3.21	2.26	4.11	2.45
K_2O	2.44	2.77	3.34	3.02	6.58	3.01	3.04	3.19	4.91	3.18	3.22
P_2O_5	0.42	0.41	0.27	0.30	0.26	0.34	0.40	0.43	0.73	0.73	0.38
Total	98.79	98.67	99.60	98.96	99.16	99.32	98.85	98.67	98.49	98	98
XRF (ppm)											
V	69	89	86	91	21	40	63	107	70	41	95
Cr	9	9	28	33	13	20	14	29	26	9	7
Ni	<6	<6	<6	<6	<6	7	<6	14	6	<5.5	7
Zn	87	103	66	80	108	59	49	79	28	54	145
Rb	390	466	419	439	524	459	550	623	482	459	510
Sr	102	94	146	141	123	74	75	102	91	126	83
Y	57	55	35	38	18	31	43	43	70	48	58
Zr	369	355	231	254	178	194	265	288	377	348	378
Nb	37	35	18	21	15	26	27	31	67	44	43
Ba	144	147	303	274	272	147	144	172	237	105	159
INA (ppm)											
Cl	428	540	680	760	210	780	800	1010	590	830	670
Sc	13.2	14.7	12.2	13.5	3.9	7.6	10.4	13.9	15.6	9.9	15.9
V	70	90	95	91	20	45	72	108	72	42	106
Cr	10	11	26	34	12	27	15	31	31	10	11
Ga	40	<50	<40	<30	<40	40	<40	<30	<30	<60	<40
Rb	396	513	428	462	540	497	550	650	510	497	476
Cs	28	36	48	48	23	38	42	48	35	36	35
Hf	10.8	10.1	7.1	7.3	5.7	6.3	8.5	7.5	12.0	9.4	10.7
Th	33.1	31.4	29.7	32.2	40.5	39.7	35.5	28.2	62.0	26.4	31.0
U	8.7	7.7	6.2	6.7	8.5	7.4	9.0	7.4	16.7	7.0	4.5
La	69	65	60	68	67	54	60	58	66	57	67
Ce	165	153	128	153	165	129	135	134	175	131	154
Nd	89	124	85	111	72	95	74	90	102	82	70
Sm	14.1	13.6	10.6	12.3	10.5	12.4	12.8	12.8	17.3	12.9	14.1
Eu	1.02	0.9	1.02	1.11	0.8	0.57	0.64	0.81	0.63	1.02	0.72
Tb	1.5	1.57	0.9	1.05	0.62	0.86	0.92	1.12	2.02	1.25	1.73
Dy	8.4	8.8	6.3	4.6	3.1	5.8	7.4	5.0	11.4	7.3	10.7
Yb	5.2	4.3	4.1	5.1	1.3	2.6	3.5	3.9	7.4	3.9	3.9
Lu	0.5	0.53	0.25	0.42	<0.4	<0.3	0.25	0.34	0.67	0.42	0.35

	Non-igneous enclaves							LAMP
	114D	208J2	208J8	229J2	230J1	230J2	237J1	236
XRF (Wt.% oxide)								
SiO_2	53.00	52.56	48.54	44.30	50.51	62.97	54.52	50.55
TiO_2	1.04	1.34	1.45	1.58	1.54	1.04	1.06	1.97
Al_2O_3	25.24	20.28	21.63	28.43	24.85	17.79	22.48	13.26
Fe_2O_3T	10.17	12.31	13.19	12.68	11.21	8.12	7.64	6.41
MnO	0.12	0.26	0.22	0.18	0.23	0.11	0.16	0.11
MgO	2.17	3.38	2.93	3.98	2.47	1.65	1.95	7.12
CaO	0.85	1.55	1.51	0.44	1.08	0.83	0.91	4.57
Na_2O	1.82	1.68	3.20	0.75	3.11	2.21	2.95	2.31
K_2O	3.82	4.26	5.14	6.00	2.18	2.92	6.25	7.1
P_2O_5	0.15	0.52	0.11	0.06	0.19	0.18	0.13	1.88
Total	98.39	98.14	97.92	98.38	97.37	97.82	98.05	95.27
XRF (ppm)								
V	175	139	164	180	149	102	139	108
Cr	129	177	184	241	145	142	117	285
Ni	44	85	15	114	31	23	42	275
Zn	230	792	185	225	125	93	190	51
Rb	968	840	1030	1113	469	644	898	257
Sr	23	39	59	19	28	19	70	1294
Y	27	46	32	62	25	26	19	27
Zr	152	288	291	360	250	346	181	1380
Nb	49	41	58	37	70	63	37	54
Ba	<30	180	212	357	<40	<34	283	5814
INA (ppm)								
Cl	390	650	1220	390	210	220	140	180
Sc	17.2	15.1	20.2	24.8	19.3	16.0	14.6	15.6
V	166	140	151	195	125	108	134	111
Cr	125	176	184	241	127	139	124	292
Ga	53	35	40	52	47	37	56	20
Rb	940	810	1080	1010	415	610	960	251
Cs	115	99	110	192	78	146	123	5
Hf	4.9	8.9	8.5	11.3	7.1	11.2	5.7	35.0
Th	19.5	20.5	27.9	23.1	28.4	24.0	17.2	49.5
U	6.7	12.0	5.0	6.6	7.7	7.3	10.9	10.8
La	49	59	57	74	60	62	51	239
Ce	106	131	127	155	130	142	111	496
Nd	41	44	59	28	66	50	39	213
Sm	9.0	11.9	9.8	13.4	11.0	11.0	8.0	24.2
Eu	0.55	0.68	0.79	1.46	0.58	0.78	1.32	5.1
Tb	0.81	1.49	0.61	1.53	0.77	0.8	0.67	1.01
Dy	2.3	8.2	3.6	9.3	<12	4.9	5.4	6.0
Yb	2.3	3.6	2.3	5.5	2.9	3.6	2.2	1.6
Lu	0.24	0.38	<0.6	0.47	0.26	<0.7	<0.5	0.28

See Appendix I for sample locations and Appendix II for analytical methods.
LAMP is the LeMail lamprophyre dyke.
Total Fe as Fe_2O_3T.

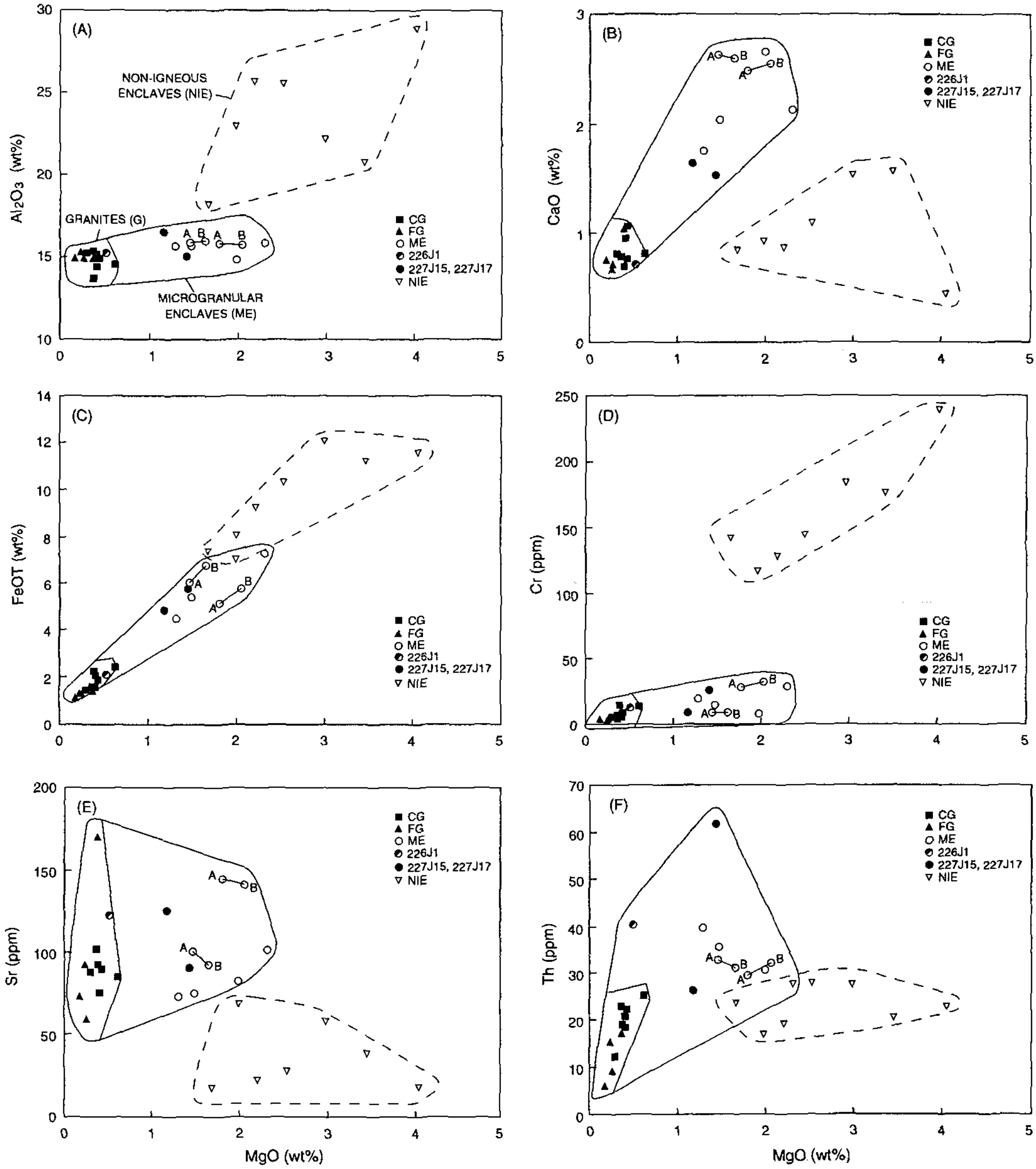

FIG. 7. Major and trace element variation diagrams for enclaves and granite host rocks analysed in this study. Whole-rock analyses normalized to 100% on an anhydrous basis (see Table 7 for raw data).

Rare-earth element (*REE*) data for the granites and their enclaves are summarized in Fig. 9. The coarse- and fine-grained granites yield overlapping patterns (Fig. 9A and B) similar to those documented in other studies of the Cornubian batholith (Darbyshire and Shepherd, 1985; Charoy, 1986; Ward *et al.*, 1992). The *REE* patterns displayed by the enclaves are similar to those of the granites, but enclaves generally have higher REE contents and larger negative Eu anomalies than their host-rocks, with ME ranging to higher values than NIE (Fig. 9C and D). The Lemail lamprophyre has a *REE* pattern typical of potassic volcanic rocks of SW England, whereas basaltic rocks of the Exeter Volcanics have

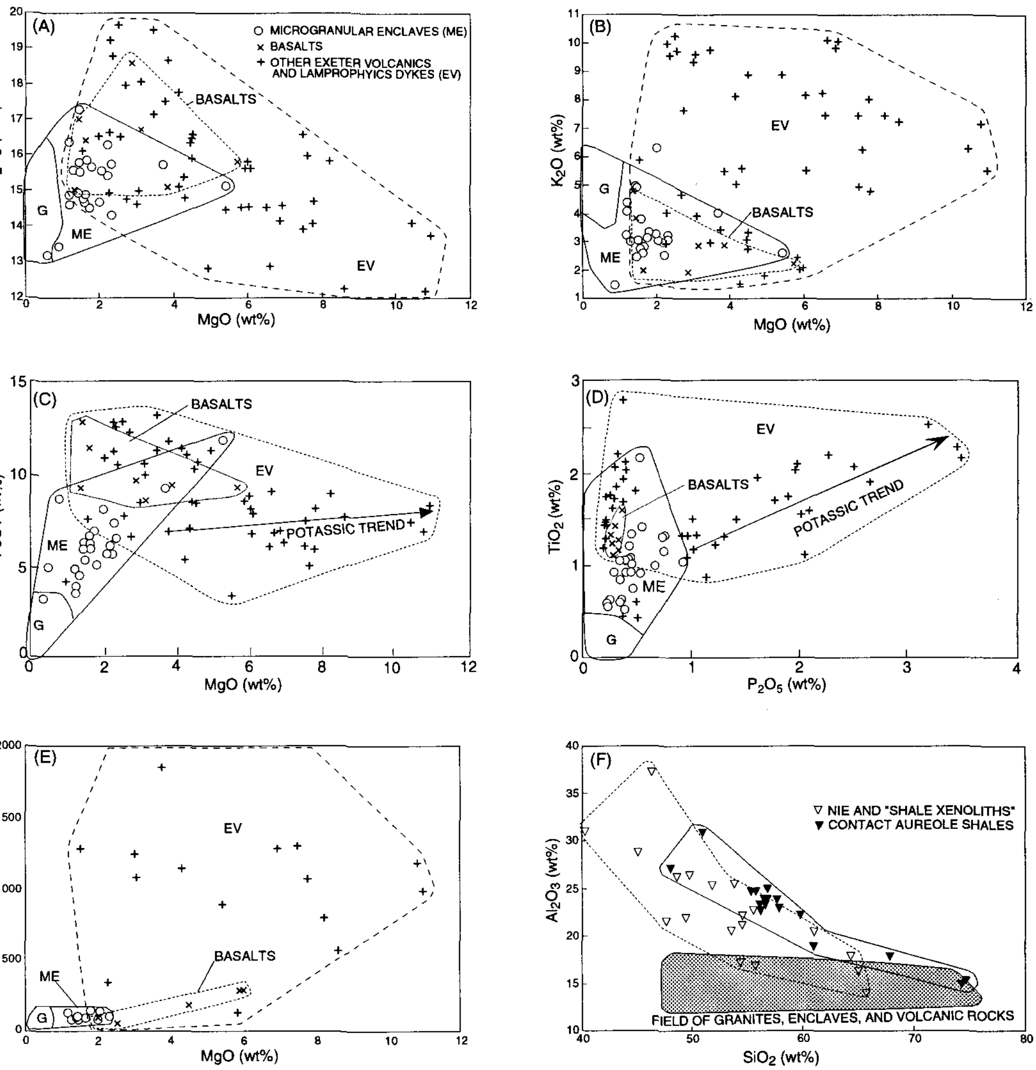

FIG. 8. Major and trace element variation diagrams for granites, enclaves, the associated Exeter Volcanics and dykes (EV), and metasedimentary rocks of the contact aureole. Basaltic rocks of the EV are distinguished from potassic rocks based on descriptions by the original investigators (data from: this study; Brammall and Harwood, 1932; Tidmarsh, 1932; Ghosh, 1928, 1934; Exley and Stone, 1982; Mitropoulos, 1982; Jefferies, 1985; Darbyshire and Sheppherd, 1985; Charoy, 1986; Leat *et al.*, 1987; Thorpe *et al.*, 1986; and Thorpe, 1987; and Ward *et al.*, 1992). Only the field of granitic rocks (G) is shown. Data normalized to 100% on an anhydrous basis.

much lower *REE* abundances (Fig. 9E). The *REE* patterns of ME do not closely resemble those of either the potassic or basaltic rocks of SW England. High *REE* contents and light *REE* enrichments relative to host granites have also been observed in other studies of microgranular (Barbarin, 1991; Orsini *et al.*, 1991) and restitic or surmicaceous (Barbey, 1991; Montel *et al.*, 1991) enclaves, and are probably due to late-stage exchange between enclaves and their host rocks, as described below.

There is considerable evidence that some rocks within the contact aureole of the Cornubian batholith have been modified by interaction with fluids derived from the granites, but there is no evidence for partial

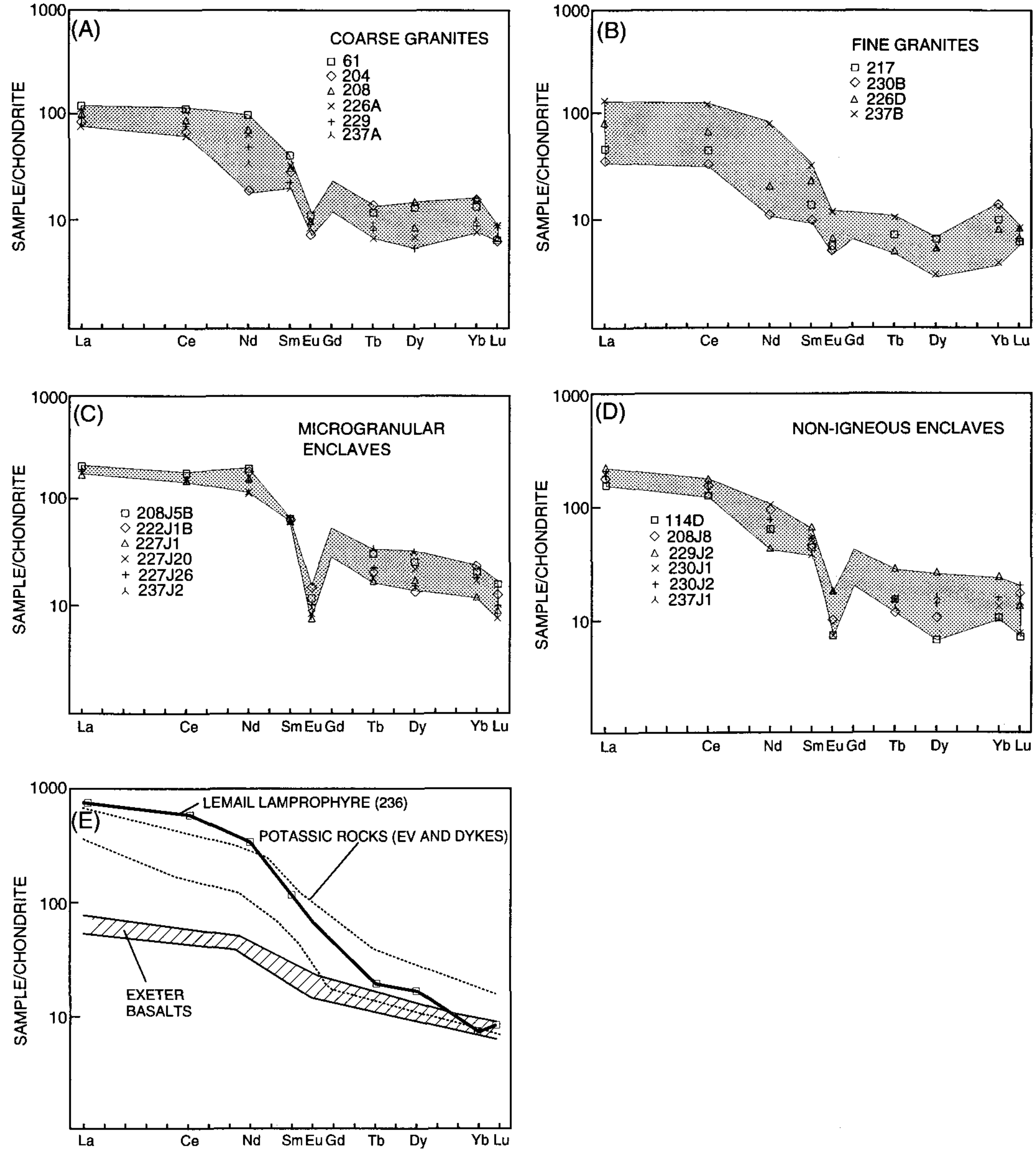

FIG. 9. Chondrite-normalized REE diagrams for granites, enclaves, and associated lamprophyre dykes and for Exeter Volcanics (for data see: Table 7 and Leat *et al.*, 1987; Thorpe *et al.*, 1986; and Thorpe, 1987). Normalization factors from Nakamura (1974).

melting at the current level of exposure (Brammall and Harwood, 1932; Mitropoulos, 1982). Overall, analyses of metasedimentary rocks from the contact aureole, 'shale xenoliths', and our NIE samples define a broad trend distinct from that of the granites and ME. That NIE are chemically unrelated to ME is especially clear in plots involving CaO, Al_2O_3 and SiO_2 (Figs. 7 and 8). A few NIE plot at even higher Al_2O_3 and lower SiO_2 than aureole shales (Fig. 8F). These NIE samples must represent the residua of partial melting at variable but higher $P-T$ conditions than that represented at the current level of exposure.

Discussion

Chemical exchange between enclaves and granitic magma

Protracted chemical exchange between enclaves and their granitic hosts renders interpretation of enclave chemistry problematic (Eberz and Nicholls, 1990; Barbarin, 1991; Orsini *et al.*, 1991; Zorpi *et al.*, 1991; van der Laan and Wyllie, 1993). Chemical modification may occur through numerous processes, summarized by Barbarin and Didier (1992). Although not all workers agree on which constituents are most affected, there is a consensus that the elements with the highest mobilities include K, Na, Cs, Rb, and Ba, whereas Fe, Mg, Ni, Cr, Zn, and V are the least mobile. Other components, including Si, Al, Ti, Ca, P, Sr, Zr, Y, Nb, Th, U, and *REE* show variable mobility.

The chemical trends of the enclaves are best understood by examining their textures and mineral assemblages. Cornubian ME consist dominantly of plagioclase, biotite, quartz, ilmenite, and lesser K-feldspar and accessory minerals. Partial re-equilibration of early-formed minerals (plagioclase, biotite and ilmenite) *via* interstitial liquid could potentially increase the concentrations of elements compatible in these phases (K, Rb, Nb, Y, Sr, Ca). The large overlaps in composition between these minerals in enclaves and their host granites (especially plagioclase and biotite) are consistent with extensive chemical exchange.

Textural relationships in some ME suggest that late-stage crystallization was dominated by growth of quartz and K-feldspar, but also included accessory minerals such as apatite, zircon, monazite and sulphides. Development of this assemblage would have the effect of increasing the concentration of silica, alkalis and incompatible elements (P, Y, Zr, Hf, Th, U, and REE). Enrichment in incompatible elements in other ME suites has been substantiated by comparison with coeval mafic plutons, which show lower (i.e. typical) abundances of these elements (Orsini *et al.*, 1991).

NIE are the residua of partial melting, consisting dominantly of aluminous minerals, biotite, plagioclase and accessory phases. Similar enclaves, interpreted as restites (Barbey, 1991; Montel *et al.*, 1991), are rich in certain incompatible (Zr, Nb, Y, U, Th, *REE* and P) and compatible elements (Mg, Ni, Cr, V, and Sc), and have variable Ca and Sr contents depending on the amount of residual plagioclase. Thus the trace element composition of NIE reflects both the high proportion of biotite, ilmenite and the accessory phases (apatite, zircon, monazite, and Fe-Cu sulphides), as well as interaction with the most magma.

Microgranular enclaves and the mafic end-member in Cornubian granite genesis

In numerous other studies mafic ME such as those observed in the Cornubian batholith have been interpreted as hybrid magmas, formed by mafic-silicic magma interaction. Detailed examination of such enclave suites in granites and rhyolites has shown that they are typically more evolved than either associated mafic plutons or lavas (Bacon, 1986; Stimac *et al.*, 1990; Zorpi *et al.*, 1991). ME are depleted in compatible elements such as Mg, Ni, Cr, Ca and Sc relative to associated mafic rocks. Moreover both the bimodal mineral assemblage (exhibiting complex disequilibrium reaction textures) and fine-grained groundmass of ME are entirely consistent with scenarios involving crystal fractionation and magma mixing/co-mingling, but are at odds with either cumulate or restite interpretations because: (1) both restites and cumulates should be enriched, not depleted, in compatible elements, and (2) cumulates should be relatively coarse-grained, with normally-zoned, equilibrium mineral assemblages.

In a simplified magma mixing model, the mafic end-member intrudes the base of a silicic system, undergoes some crystal fractionation prior to or concurrently with mixing, and eventially produces magma with intermediate composition in a hybrid layer. This intermediate magma subsequently intrudes higher levels of the silicic system, forming enclaves (Stimac and Pearce, 1992). In such a situation, the mafic end-member of the system will rarely be preserved in the upper portions of a plutonic complex, and extrapolation of the linear trends defined by the enclaves and host granites will lead to underestimation of the concentrations of compatible elements in the mafic end-member.

We have shown above that ME in the Cornubian batholith are distinct from NIE and have textures and compositions consistent with partial quenching of hybrid intermediate magmas, later modified by exchange with the hosting granitic magmas. Evidence for such an origin includes: (1) the igneous mineralogy and fine-grained texture typical of ME, suggestive of rapid (undercooled) crystallization of a relatively mafic magma; (2) the occurrence of scarce, medium-grained, crystal aggregates of labradorite and Mg-rich biotite in some ME, which probably represent phenocrysts from more mafic magmas; (3) the presence of coarse-grained feldspar, quartz and biotite crystals in ME, which are the same size and composition as phenocrysts in the host granite, and exhibit reaction textures typical of silicic xenocrysts in mixed magmas; (4) the fact that ME define broadly linear arrays (for immobile elements) that extend from the host granite trend to considerably more mafic compositions; and (5) the observation that lines connecting paired samples from heterogeneous and composite enclaves generally parallel those arrays.

The origin of large K-feldspar crystals in ME deserves special attention because in southwest England such occurrences have been widely interpreted as a result of metasomatism (Stone and Austin, 1961; Exley and Stone, 1964, 1982; Al-Turki, 1972). This interpretation was based in part on the assumption that enclaves were solid rocks (i.e. country-rock, basic igneous xenoliths, or restitic material) at the time of incorporation. The evidence cited in these studies includes the occurrence of megacrysts inside or straddling enclave–granite contacts or cutting aplite–granite contacts. However, K-feldspar megacrysts are nowhere present in NIE, as would be expected if late metasomatic growth had occurred. Moreover, ME containing K-feldspar megacrysts also contain coarse-grained plagioclase and biotite similar in composition to phenocrysts in the host granites (Figs. 5 and 6). These textural and compositional relationships are entirely consistent with formation of microgranular enclaves by magma mixing, the coarse-grained minerals being derived from the silicic end-member magma (cf. Hibbard, 1981; Vernon, 1990). K-feldspar megacrysts in many Cornubian granites and ME also contain rounded interfaces and zones with inclusions of plagioclase, biotite and quartz. Such features are typical of the complex crystallization histories of magmatic feldspar (Vernon, 1983; Stimac and Pearce, 1992). Moreover, K-feldspar megacrysts in microgranular enclaves are commonly mantled by plagioclase (An_{14-27}), whereas similar mantles are essentially absent in the granite host (cf. Brammall and Harwood, 1932; Fig. 3F). Such rapakivi mantles on K-feldspar are common in enclave-rich hybrid magmas, and form in response to the mixing process (Hibbard, 1981; Bussy, 1990; Vernon, 1990; Stimac and Wark, 1992), but are inconsistent with the concept that K-feldspar formed by late metasomatic growth.

A connexion between Cornubian granites and basaltic rocks of the Exeter Volcanics was advocated by Tidmarsh (1932), who considered some basalts to represent mixtures of mantle-derived magmas and granitic magmas of the batholith. The composition and mineralogy of ME sampled in this study do not establish a definitive link to either the basaltic or potassic rocks volcanic rocks of SW England, but suggest that ME are more closely affiliated with the basalts than the strongly potassic rocks. Potential mixing arrays defined by the granites and ME project into the field defined by lamprophyres and basalts, but more closely parallel the trends of the basaltic rocks (Fig. 8). However, it is clear that relative to any parent basalt, ME compositions have been considerably modified through crystal fractionation, magma mixing, and subsequent interaction with their granitic hosts. In particular, ME are: (1) depleted in compatible elements, probably due to fractionation of olivine and clinopyroxene; and (2) enriched in incompatible elements such as Hf, Y, Th, U and *REE*, probably due to late crystallization of incompatible-rich accessory phases in the enclaves, stimulated by chemical exchange with their granite host magmas. Although these latter enrichments may also be suggestive of lamprophyric affinities (e.g. Ayrton, 1991), the extreme mismatch between ME and the potassic rocks for many elements make this possibility unlikely.

The sparsity of ME in the Cornubian granites may reflect the highly evolved composition and shallow erosional level of the batholith. Nevertheless, the existence of ME in even trace amounts confirms that coeval mafic magmas played a role in the evolution, and probably in the origin of the granites. The fact that such enclaves are present in all of the major plutons except Carnmenellis suggests that mafic input occurred over essentially the entire spatial and temporal range of the batholith (Clark *et al.*, 1993). The importance of basaltic injection in the origin of granitic magmas has been stressed by a number of workers on the basis of physical, chemical and textural arguments (Hildreth, 1981; Huppert and Sparks, 1988). Addition of mantle-derived heat provides an explanation for large-volume crustal melting in regions of relatively thin crust such as southwest England (Stone and Exley, 1986; Willis-Richards and Jackson, 1989).

Non-igneous enclaves (NIE)

Individual NIE in the Cornubian granites have mineral assemblages that provide broad constraints on their *T* and *P* of formation, and imply that they have suffered variable degrees of partial melting and melt extraction. NIE containing coarse-grained muscovite preserve evidence for the reactions:

$$\text{Ms} + \text{Crd} \rightarrow \text{And} + \text{Bt} + \text{Qtz} + H_2O, \qquad (1)$$

or

$$\text{Ms} + \text{Qtz} \rightarrow \text{And} + \text{Kf} + H_2O, \qquad (2)$$

which generated enclaves rich in andalusite, biotite and quartz (e.g. 229J2). At least one such enclave contains leucosomes that may represent trapped melt (237J1). A few NIE consist of strongly silica-deficient layers containing cordierite, hercynite, corundum and biotite. Similar assemblages are common in the inner domains of high-*T*, moderate-*P*, contact aureoles (Pattison and Harte, 1989; Grant and Frost, 1990) and the melanosomes of migmatites (e.g. Harris, 1981). Textural relationships suggest that corundum in these enclaves formed by the reactions:

$$\text{Bt + Sil + Pl Kf } H_2O \rightarrow \text{Crd + Herc + Cor + L}, \quad (3)$$
$$\text{Herc + Sil} \rightarrow \text{Crd + Cor}, \quad (4)$$

during progressive anatexis. These NIE may represent fragments derived from unexposed levels of the contact aureole or restite from the region of magma generation. The high Al_2O_3, Cr and MgO, and low SiO_2, CaO and K_2O contents of some NIE are plausibly ascribed to extraction of partial melts. As described by Harris (1981), anatexis reduces the SiO_2, alkali, and H_2O contents in the residuum: free silica is lost when the composition reaches the cordierite–garnet–sillimanite plane in the system Al_2O_3–SiO_2–FeO–MgO, while, with further melting, garnet is consumed and the remaining phases are joined by spinel and, finally, by corundum. The absence of garnet in all of our NIE samples could indicate either that garnet was destroyed through reactions such as:

$$\text{Gar + Sil} \rightarrow \text{Crd + Herc}, \quad (5)$$

or that all such enclaves were metamorphosed at pressures below the stability of garnet. It should, however, be noted that rare garnet-bearing granite and enclaves have been reported from the Dartmoor pluton (Brammall and Harwood, 1932). Stone (1990) re-examined these samples and concluded that garnet and cordierite were restitic, implying a depth of magma generation between 18 and 25 km ($\sim$ 6–8 kbar).

Overall, NIE have a range of compositions, textures and mineral assemblages suggesting higher (but variable) *T* and *P* of formation than those of the exposed contact aureoles. The common occurrence of andalusite-only, andalusite + fibrolite, or sillimanite-only assemblages suggest that most NIE equilibrated at relatively low pressures, at or below the aluminosilicate triple point ($\leqslant$ 4.5 kbar: Pattison, 1992). It is probable that observed NIE in Cornubian granites were derived from depths ranging from the site of anatexis, for which *T* and *P* have been estimated at $\sim$ 800°C and 5 kbar by Charoy (1986), to near the current level of exposure [*T* and *P* estimated at 520–540°C and 1 kbar based on aureole assemblages by Floyd (1971) and $\sim$650°C and 2.0–2.5 kbar based on mineral assemblages in the granites by Charoy (1986)]. We observe no clear relation between the textures and mineral assemblages in the aureole and those of NIE, and thus find it unlikely that NIE were derived from the current level of exposure as was suggested by Ghosh (1928, 1934) and Lister (1984).

Conclusions

Enclaves of both igneous (ME) and metamorphic origin (NIE) are present in trace amounts in the coarse-grained biotite granites of the Cornubian batholith. Enclaves of igneous origin can be distinguished from enclaves of restitic material and thermally metamorphosed country-rock by their microgranular texture, low Al_2O_3, high CaO and the mineral assemblage, plagioclase, biotite, quartz $\pm$ K-feldspar, opaques, and apatite $\pm$ cordierite. In contrast, enclaves of metamorphic origin are layered, high in Al_2O_3 and low in CaO, and contain abundant aluminosilicates, corundum, cordierite and biotite.

NIE have a range of mineral assemblages and compositions suggesting various degrees of melt extraction and variable metamorphic conditions. Rare NIE containing the highest-grade assemblages (sillimanite–hercynite–corundum–biotite) may be truly restitic, whereas more typical NIE containing andalusite but no sillimanite may represent either re-equilibrated restitic material or thermally metamorphosed country-rock from levels deeper than the present level of exposure.

ME define a broad compositional range from granite to tonalite and do not preserve direct mineralogic evidence of either a basaltic or lamprophyric component. In the light of the textural evidence for the hybrid origin of the ME, chemical trends are taken to represent mixing arrays between biotite granite and an unobserved end-member of mafic composition, significantly modified by host-enclave exchange for some elements. The large disparity in concentrations of K, P, Ba, Rb, Sr, Ni and Cr between the enclave-granite array and the field of the more potassic rocks of the coeval Exeter Volcanics implies that the ME were probably derived from a basaltic rather than a lamprophyric parent (Fig. 8). Partially reacted megacrysts of K-feldspar, plagioclase, quartz and biotite are common in ME, but entirely absent in enclaves of metamorphic origin. Textural and chemical evidence indicates that K-feldspar megacrysts in the enclaves were derived from the silicic end-member in the course of magma mixing, and not from metasomatic processes.

The presence of microgranular enclaves in granites ranging in age from 275 to 290 Ma (Chen *et al.*, 1993), and the occurrence of coeval lamprophyric dykes and the basaltic to lamprophyric Exeter Volcanics, suggest that heat added to the deep crust by injection of mantle-derived magmas may have been a factor in the generation of the Cornubian batholith, as in other sites of large-volume crustal melting in regions of relatively thin crust.

Acknowledgements

Field expenses and a part of the laboratory costs were contributed by Natural Sciences and Engineering Research Council of Canada operating grants to A.H.C. NSERC also supported J.A.S as a post-doctoral research fellow for a period of 6 months. Frank Lucas, Keith Atkinson, Alan Bromley and Richard Scrivenor provided advice, encouragement and logistical support during the field work. Walter Morales helped with sample preparation. Invaluable assistance with manuscript preparation was given by Joan Charbonneau. James Archuleta and Eric Montoya prepared the figures. J.A.S. was a Director's Post-Doctoral Fellow at Los Alamos National Laboratory while completing this study. Reviews by F. Goff, B. Barbarin and an anonymous reviewer improved an earlier version of this manuscript.

APPENDIX I. Sample Locations

Sample	Description	Location/Pluton	Latitude	Longitude
61	CG	Lamorna Cove, LE	50°03′52″N	5°33′48″W
114D	NIE	Kessel Quarry, CM	50°09′35″N	5°1′00″W
204	CG	Pewtor, DM	50°32′24″N	4°0′20″W
208	CG	Luxulyan Quarry, SA	50°23′50″N	4°44′25″W
208J2	NIE			
208J5	ME			
208J8	NIE			
217	FG	Castle-An-Dinas, LE	50°09′30″N	5°31′10″W
222J1	ME	Birch Tor, DM	50°36′44″N	3°51′50″W
226A	CG	Peninnis Cove, SI	49°54′15″N	6°18′10″W
226D	FG			
226J1	ME			
227J1	ME	Sennen Cove, LE	50°04′41″N	5°42′15″W
227J15	ME			
227J17	ME			
227J20	ME			
227J26	ME			
229A	CG	Carnsew Quarry, CM	50°10′05″N	5°08′20″W
229B	FG			
229J1	NIE			
230A	CG	Chywoon Quarry, CM	50°10′10″N	5°09′15″W
230B	FG			
230J1	NIE			
230J2	NIE			
236	LAMP	Lemail lamprophyre	50°31′24″N	4°47′27″W
237A	CG	De Lank Quarry, BM	50°32′47″N	4°40′50″W
237B	FG			
237J1	NIE			
237J2	ME			

LE, Land's End pluton; CM, Carnmenellis; DM, Dartmoor; SA, St. Austell; BM, Bodmin Moor; SI, Isles of Scilly; CG, Coarse-grained granitoid; FG, fine-grained granitoid; ME, microgranular enclave; NIE, non-igneous enclave; LAMP, lamprophyre.

Appendix II. Analytical methods

Field, chemical and textural study of the granites and their enclaves was limited by poor exposure, and extensive alteration due to late-stage and post-emplacement processes. Alteration includes locally quasi-pervasive kaolinization and greisening. Special efforts were made to obtain pristine material, but in some cases the paucity of enclaves dictated examination of slightly altered rocks. Microgranular enclaves are most affected by sericitization and chloritization, whereas enclaves with metamorphic textures are affected primarily by tourmalinization.

Samples were crushed in a steel jaw crusher and pulverized in a tungsten carbide shatterbox. Duplicate discs for X-ray fluorescence analysis were prepared by fusing 3.000 $\pm$ 0.005 g of sample and 6.000 $\pm$ 0.005 g of Li-metaborate flux in graphite crucibles at 1150°C for 40–60 minutes. The surfaces of the fused discs were then ground flat and polished. Duplicate samples were analyzed for major elements (Si, Ti, Al, Fe, Mn, Mg, Ca, Na, K, and P) and selected trace elements (Ba, Rb, Sr, V, Cr, Ni, Zn, Y, Zr, and Nb) with a Rigaku 3064 Dataflex X-Ray fluorescence spectrometer at Los Alamos National Laboratory. Data reduction was accomplished by the 'fundamental parameters' method (Criss, 1980) which applies X-ray absorption and secondary fluorescence corrections to a set of standard intensities. Analyses of standards indicate that 2σ precision is generally 2–3% for major elements except Mn and P (5–10%), and 2–3% at concentrations of > 50 ppm for trace elements. Accuracy is typically within 5–10% for Sr, Zn, Rb, V, Zr, and Y, and from 15 to 25% for Ba, Cr, Nb, and Ni at concentrations of > 50 ppm. Both precision and accuracy are poorer near detection limits, especially for Ba, Cr, Ni, and Nb.

Neutron activation analyses were carried out at the automated Los Alamos National Laboratory Omega West Reactor. Vials containing approximately 4 g of sample were weighed on a computerized balance, and exposed to a neutron flux of $\sim 6 \times 10^{12}$n/s/cm^2 for 20 s. Samples were counted at 20 min, 7 days, and 2–3 weeks to measure both short- and long-lived radionuclides. The data were acquired via four Ge(Li) gamma-ray detectors, each with FWHM at 1332 keV of approximately 2.1 keV, and reduced on a PDP-11/60 computer using a program, 'Raygun', which fits peaks and backgrounds and corrects for overlaps. Standard analysis indicates that the system yields 1σ standard deviation of < 5% for isotopes well above detection limit. A '<' sign preceding values listed in Table 7 signifies minimum detection limits for that element in a given sample.

Microanalyses of minerals were obtained using a Cameca MBX electron microprobe operating at 15 kV accelerating potential and 0.015 µA sample current. Data were calculated using a Bence-Albee reduction scheme. Calibration for WDS analysis was achieved using appropriate mineral standards, and checked by analysis of secondary standards.

References

Al-Turki, K. (1972) *A Petrographic and Chemical Study of the Carnmenellis Granite and Associated Rocks.* Unpubl. Ph.D. thesis, University of Exeter.

Ayrton, S. N. (1991) Appinites, lamprophyres and mafic magmatic enclaves: three related products of interaction between acid and mafic magmas. In *Enclaves and Granite Petrology* (Didier, J. and Barbarin, B., eds.). Developments in Petrology, **13**, Amsterdam: Elsevier, 465–78.

Bacon, C. R. (1986) Magmatic inclusions in silicic and intermediate volcanic rocks. *J. Geophys. Res.*, **91**, 6091–112.

Barbarin, B. (1991) Enclaves of the Mesozoic calc-alkaline granitoids of the Sierra Nevada batholith, California. In *Enclaves and Granite Petrology* (Didier, J. and Barbarin, B., eds.). Developments in Petrology, **13**, Amsterdam: Elsevier, 135–54.

Barbarin, B. and Didier, J. (1992) Genesis and evolution of mafic microgranular enclaves through various types of interaction between coexisting felsic and mafic magmas. *Trans. Royal Soc. Edinburgh*, **83**, 145–53.

Barbey, P. (1991) Restites in migmatites and autochthonous granites: Their main features and their genesis. In *Enclaves and Granite Petrology* (Didier, J. and Barbarin, B., eds.). Developments in Petrology, **13**, Amsterdam: Elsevier, 479–92.

Brammall, A. and Harwood, H. F. (1932) The Dartmoor granites: their genetic relationships. *Q. J. Geol. Soc. London*, **88**, 171–237.

Bromley, A. (1989) Field Guide to the Cornubian Orefield. In *6th International Symposium on Water–Rock Interaction* (Malvern, UK), Camborne School of Mines, 111 pp.

Bussy, F. (1990) The rapakivi texture of feldspars in a plutonic mixing environment: a dissolution-recrystallization process? *Geol. J.*, **25**, 319–24.

Chappell, B. W. and White, A. J. R. (1992) I- and S-type granites in the Lachlan Fold Belt. *Trans. Royal Soc. Edinburgh*, **83**, 1–26.

Chappell, B. W., White, A. J. R. and Wyborn, D. (1987) The importance of residual source material (restite) in granite petrogenesis. *J. Petrol.*, **28**, 1111–38.

Charoy, B. (1986) The genesis of the Cornubian Batholith (South-West England): the example of the Carnmenellis Pluton. *J. Petrol.*, **27**, 571–604.

Chen, Y., Clark, A. H., Farrar, E., Wasteneys, H. A. H. P., Hodgson, M. J. and Bromley, A. V. (1993) Diachronous and independent histories of plutonism and mineralisation in the Cornubian Batholith, SW England. *J. Geol. Soc. London*, **150**, 1183–91.

Chesley, J. T., Halliday, A. N., Snee, L. W., Mezger, K., Shepherd, T. J. and Scrivener, R. C. (1993) Thermochronology of the Cornubian batholith in southwest England: implications for pluton emplacement and protracted hydrothermal mineralization. *Geochim. Cosmochim. Acta*, **57**, 1817–35.

Clark, A. H., Chen, Y., Farrar, E., Wasteneys, H. A. H. P., Stimac, J. A., Hodgson, M. J., Willis-Richards, J.

and Bromley, A. V. (1993) The Cornubian Sn-Cu (-As, W) metallogenetic province: product of a 30 m.y. history of discrete and concomitant anatectic, intrusive and hydrothermal events. *Proc. Ussher Soc.*, **8**, 112–6.

Criss, J. (1980) 'Fundamental parameters' calculations on a laboratory microcomputer. In: *Advances in X-Ray Analysis*, **23**, 93–7.

Dangerfield, J. and Hawkes, J. R. (1981) The Variscan granites of SW England: additional information. *Proc. Ussher Soc.*, **5**, 116–20.

Darbyshire, D. P. F. and Shepherd, T. J. (1985) Chronology of granite magmatism and associated mineralization, SW England. *J. Geol. Soc. London*, **142**, 1159–77.

De La Beche, H. T. (1839) Report on the Geology of Cornwall, Devon, and West Somerset: *Mem. Geol. Surv.*, London: Longman, Orme, Brown, Green, and Longmans.

Didier, J. (1973) *Granites and their Enclaves: The Bearing of Enclaves on the Origin of Granites.* Developments in Petrology, **3**, Amsterdam: Elsevier, 393 pp.

Didier, J. and Barbarin, B., eds. (1991*a*) *Enclaves and Granite Petrology*, Developments in Petrology, **13**, Amsterdam, Elsevier, 625 pp.

Didier, J. and Barbarin, B. (1991*b*) The different types of enclaves in granites — nomenclature. In *Enclaves and Granite Petrology* (Didier, J. and Barbarin, B., eds.). Developments in Petrology, **13**, Amsterdam: Elsevier, 19–23.

Eberz, G. W. and Nicholls, I. A. (1990) Chemical modification of enclave magma by post-emplacement crystal fractionation, diffusion, and metasomatism. *Contrib. Mineral. Petrol.*, **104**, 47–55.

Exley, C. S. and Stone, M. (1964) The Granitic Rocks of South-west England. In *Present Views of Some Aspects of the Geology of Cornwall and Devon* (Hosking, K. F. G. and Shrimpton, G. J., eds.), Royal Geological Society of Cornwall, 131–84.

Exley, C. S. and Stone, M. (1982) Hercynian intrusive rocks. In *Igneous Rocks of the British Isles* (Sutherland, D. S. ed.), J. Wiley and Sons, 287–320.

Floyd, P. A. (1971) Temperature distribution in the Land's End granite aureole, Cornwall. *Proc. Ussher Soc.*, **2**, 335–51.

Ghosh, P. K. (1928) Petrology of the Bodmin Moor granite, Cornwall. *Mineral. Mag.*, **21**, 285–309.

Ghosh, P. K. (1934) The Carnmenellis granite: its petrology, metamorphism and tectonics. *Q. J. Geol. Soc. London*, **90**, 240–76.

Grant, J. A. and Frost, B. R. (1990) Contact metamorphism and partial melting of pelitic rocks in the aureole of the Laramie anorthosite complex, Morton Pass, Wyoming. *Amer. J. Sci.*, **290**, 425–72.

Hall, A. (1974) Granite porphyries in Cornwall. *Proc. Ussher Soc.*, **3**, 145–9.

Harris, N. (1981) The application of spinel-bearing metapelites to P/T determinations: an example from South India. *Contrib. Mineral. Petrol.*, **76**, 229–33.

Hibbard, M. J. (1981) The magma mixing origin of mantled feldspars. *Contrib. Mineral. Petrol.*, **76**, 158–70.

Hildreth, W. (1981) Gradients in silcic magma chambers: implications for lithospheric magmatism. *J. Geophys. Res.*, **86**, 10153–92.

Huppert, H. H. and Sparks, S. J. (1988) The generation of granitic magmas by intrusion of basalt into continental crust. *J. Petrol.*, **29**, 599–624.

Jefferies, N. L. (1985) The origin of sillimanite-bearing pelitic xenoliths within the Carnmenellis pluton, Cornwall. *Proc. Ussher Soc.*, **6**, 229–36.

Knill, D. C. (1969) The Permian igneous rocks of Devon. *British Geol. Surv. Bull. 29*, 115–38.

Knill, D. C. (1982) Permian volcanism in south-western England. In *Igneous Rocks of the British Isles* (Sutherland, D. S., ed.). J. Wiley and Sons, 329–32.

Leat, P. T., Thompson, R. N., Morrison, M. A., Hendry, G. L. and Trayhorn, S. C. (1987) Geodynamic significance of post-Variscan intrusive and extrusive potassic magmatism in SW England. *Trans. R. Soc. Edinburgh: Earth Sci.*, **77**, 349–60.

Lister, C. J. (1984) Xenolith assimilation in the granites of south-west England. *Proc. Ussher Soc.*, **6**, 46–53.

Miller, J. A., Shibata, K. and Munro, M. (1962) The potassium-argon age of the lava of Killerton Park, near Exeter. *Geophys. J.*, **6**, 394–6.

Mitropoulos, P. (1982) REE patterns of the metasedimentary rocks of the Land's End granite aureole (southwest England). *Chem. Geol.*, **35**, 265–80.

Montel, J. M., Didier, J. and Pichavant, M. (1991) Origin of surmicaceous enclaves in intrusive granites. In *Enclaves and Granite Petrology* (Didier, J. and Barbarin, B., eds.). Developments in Petrology, **13**, Amsterdam: Elsevier, 509–28.

Nakamura, N. (1974) Determination of REE, Ba, Mg, Na and K in carbonaceous and ordinary chondrites. *Geochim. Cosmochim. Acta* **38**, 757–75.

Orsini, J. B., Cocirta, C and Zorpi, M. J. (1991) Genesis of mafic microgranular enclaves through differentiation of basic magmas, mingling and chemical exchanges with their host granitoid magmas. In *Enclaves and Granite Petrology* (Didier, J. and Barbarin, B., eds.). Developments in Petrology, **13**, Amsterdam: Elsevier, 445–64.

Osman, C. W. (1928) The granites of the Scilly Isles and their relation to the Dartmoor granites. *Q. J. Geol. Soc. London*, **84**, 258–92.

Pattison, D. R. M. (1992) Stability of andalusite and sillimanite and the Al_2SiO_5 triple point: constraints from the Ballachulish Aureole, Scotland. *J. Geol.*, **100**, 423–46.

Pattison, D. R. M. and Harte, B. (1989) A petrogenetic grid for pelities in the Ballachulish aureole and other

Scottish thermal aureoles. *J. Geol. Soc. London*, **142**, 7–28.

Reid, C., Barrow, G., Sherlock, R., L., MacAlister, D. A., Dewey, H. and Bromehead, C. N. (1912) The Geology of Dartmoor. *Memoir of the Geological Survey of England and Wales*, Sheet 338, 102 pp.

Robson, J. (1964) The Cornish 'Greenstones'. In *Present Views of Some Aspects of the Geology of Cornwall and Devon* (Hosking, K. F. G. and Shrimpton, G. J., eds.), Royal Geological Society of Cornwall, 115–30.

Stimac, J. A. and Pearce, T. H. (1992) Textural evidence of mafic-felsic magma interaction in dacitic lavas, Clear Lake, California. *Amer. Mineral.*, **77**, 795–809.

Stimac, J. A., Pearce, T. H., Donnelly-Nolan, J. M. and Hearn, B. C. (1990) Origin and implications of undercooled andesitic inclusions in rhyolites, Clear Lake, California. *J. Geophys. Res.*, **95**, 17729–46.

Stimac, J. A. and Wark, D. A. (1992) Plagioclase mantles on sanidine in silicic lavas, Clear Lake, California: Implications for the origin of rapakivi texture. *Geol. Soc. Amer. Bull.*, **104**, 728–44.

Stone, M. (1990) The significance of almandine garnets in the Lundy and Dartmoor granites. *Mineral. Mag.*, **52**, 651–8.

Stone, M. (1992) The Tregonning granite: petrogenesis of Li-mica granites in the Cornubian batholith. *Mineral. Mag.*, **56**, 141–55.

Stone, M. and Austin, W. G. C. (1961) The metasomatic origin of the potash feldspar megacrysts in the granites of southwest England. *J. Geol.*, **69**, 464–72.

Stone, M. and Exley, C. S. (1986) High heat production granites of Southwest England and their associated mineralization: a review. In *High Heat Production (HHP) Granites, Hydrothermal Circulation and Ore Genesis*, Inst. Min. Metall., London, 571–93.

Stone, M. and Exley, C. S. (1989) Geochemistry of the Isles of Scilly pluton. *Proc. Ussher Soc.*, **7**, 152–7.

Thorpe, R. S. (1987) Permian K-rich volcanic rocks of Devon: petrogenesis, tectonic setting and geological significance. *Trans. Roy. Soc. Edinburgh: Earth Sci.*, **77**, 361–6.

Thorpe, R. S., Cosgrove, M. E. and Van Calsteren, P. W. C. (1986) Rare earth element, Sr-and Nd-isotope evidence for petrogenesis of Permian basaltic and K-rich volcanic rocks from south-west England. *Mineral. Mag.*, **50**, 481–90.

Tidmarsh, W. G. (1932) The Permian lavas of Devon. *Q. J. Geol. Soc. London*, **88**, 712–75.

Ussher, W. A. E. (1902) The geology of the country around Exeter (sheet 325). *Mem. Geol. Surv. U.K.* (London: HMSO).

van der Laan, S. R. and Wyllie, P. J. (1993) Experimental interaction of granitic and basaltic magmas and implications for mafic enclaves. *J. Petrol.* **34**, 491–517.

Vernon, R. H. (1983) Restite, xenoliths, and microgranitoid enclaves in granites. *J. Proc. Royal Soc. New South Wales*, **116**, 77–103.

Vernon, R. H. (1990) Crystallization and hybridism in microgranitoid enclave magmas: microstructural evidence. *J. Geophys. Res.*, **95**, 17849–17859.

Ward, C. D., McArthur, J. M. and Walsh, J. N. (1992) Rare earth element behaviour during evolution and alteration of the Dartmoor granite, SW England. *J. Petrol.*, **33**, 785–815.

Willis-Richards, J. and Jackson, N. J. (1989) Evolution of the Cornubian ore field, southwest England: Part I. Batholith modeling and ore distribution. *Econ. Geol.*, **84**, 1078–100.

Zorpi, M. J., Coulon, C. and Orsini, J. B. (1991) Hybrization between felsic and mafic magmas in calc-alkaline granitoids — a case study in northern Sardinia, Italy. *Chem. Geol.*, **92**, 45–86.

[*Manuscript received 12 January 1994: revised 9 September 1994*]